Ehrenfest+R Dynamics: A Mixed Quantum-Classical Electrodynamics Simulation of Spontaneous Emission

Hsing-Ta Chen,[1, a)] Tao E. Li,[1] Maxim Sukharev,[2, 3] Abraham Nitzan,[1] and Joseph E. Subotnik[1]
[1)] *Department of Chemistry, University of Pennsylvania, Philadelphia, Pennsylvania 19104, U.S.A.*
[2)] *Department of Physics, Arizona State University, Tempe, Arizona 85287, USA*
[3)] *College of Integrative Sciences and Arts, Arizona State University, Mesa, AZ 85212, USA*

The dynamics of an electronic system interacting with an electromagnetic field is investigated within mixed quantum-classical theory. Beyond the classical path approximation (where we ignore all feedback from the electronic system on the photon field), we consider all electron–photon interactions explicitly according to Ehrenfest (i.e. mean–field) dynamics with coupled Maxwell–Liouville equations. Because Ehrenfest dynamics cannot capture certain quantum features of the photon field correctly, we propose a new *Ehrenfest+R* method that can recover (by construction) spontaneous emission while also distinguishing between electromagnetic fluctuations and coherent emission.

I. INTRODUCTION

Light–matter interactions are of pivotal importance to the development of physics and chemistry. The optical response of matter provides a useful tool for probing the structural and dynamical properties of materials, with one possible long term goal being the manipulation of light to control microscopic degrees of freedom. Now, we usually describe light–matter interactions through linear response theory; the electromagnetic (EM) field is considered a perturbation to the matter system and the optical response is predicted by extrapolating the behavior of the system without illumination. Obviously, this scheme does not not account for the feedback of the matter system on the EM field, and many recent experiments can not be modeled through this lens. For instance, in situations involving strong light–matter coupling, such as molecules in an optical cavity, spectroscopic observations of nonlinearity have been reported as characteristic of quantum effects.[1–3] As another example, for systems composed of many quantum emitters, collective effects from light–matter interactions lead to very different phenomena from linear response theory, such as coupled exciton–plasma optics[4–7] and superradiance lasers.[8–10]

The phenomena above raise an exciting challenge to existing theories; one needs to treat the matter and the EM field within a consistent framework. Despite our great progress heretofore using simplified quantum models,[11,12] semiclassical simulations provide an important means for studying subtle light–matter interactions in realistic systems.[13] Most semiclassical simulations are based on a mixed quantum–classical separation treating the electronic/molecular system with quantum mechanics and the bath degrees of freedom with classical mechanics. While there are many semiclassical approaches for coupled electronic–nuclear systems offering intuitive interpretations and reliable predictions,[14–17] the feasibility of analogous semiclassical techniques for coupled electron–radiation dynamics remains an open question. With that in mind, recent semiclassical advances, including numerical implementation of the Maxwell–Liouville equation,[18–21] symmetrical quantum-classical dynamics,[22,23] and mean-field Ehrenfest dynamics,[23] have now begun exploring exciting collective effects, even when spontaneous emission is included.

For electron–radiation dynamics, the most natural approach is the Ehrenfest method, combining the quantum Liouville equation with classical electrodynamics in a mean-field manner; this approach should be reliable given the lack of a time-scale separation between electronic and EM dynamics. Nevertheless, Ehrenfest dynamics are known to suffer from several drawbacks. First, it is well-known that, for electronic–nuclear dynamics, Ehrenfest dynamics do not satisfy detailed balance.[24] This drawback will usually lead to incorrect electronic populations at long times. The failure to maintain detailed balance results in anomalous energy flow (that can even sometimes violate the second law of thermodynamics at equilibrium.[25]) For electron–radiation dynamics, this problem may not be fatal since the absorption and emission of a radiation field may be considered relatively fast compared to electronic–nuclear dynamics.

Apart from any concerns about detail balance, Ehrenfest dynamics has a second deficiency related to spontaneous and stimulated emission.[23] Consider a situation where the electronic system has zero average current initially and exists within a vacuum environment without external fields; if the electronic state is excited, one expects spontaneous emission to occur. However, according to Ehrenfest dynamics, the electron–radiation coupling will remain zero always, so that Ehrenfest dynamics will not predict any spontaneous emission. In this paper, our goal is to investigate the origins of this Ehrenfest failure by analyzing the underlying mixed quantum–classical theory; even more importantly we will propose a new *ad hoc* algorithm for adding spontaneous emission into an Ehrenfest framework.

[a)] Electronic mail: hsingc@sas.upenn.edu

This paper is organized as follows. In Sec. II, we review the quantum electrodynamics (QED) theory of spontaneous emission. In Sec. III, we review Ehrenfest dynamics as an anstaz for semiclassical QED and quantify the failure of the Ehrenfest method to recover spontaneous emission. In Sec. IV, we propose a new Ehrenfest+R approach to correct some of the deficiencies of the standard Ehrenfest approach. As a demonstration, Sec. V presents Ehrenfest+R results for spontaneous emission emanating from a two-level system in 1D and 3D space. In Sec. VI, we discuss extensions of the proposed Ehrenfest+R approach, including applications to energy transfer and Raman spectroscopy.

In this paper, we use a bold symbol to denote a space vector $\mathbf{r} = x\hat{\mathbf{x}} + y\hat{\mathbf{y}} + z\hat{\mathbf{z}}$ in Cartesian coordinate. Vector functions are denoted as $\mathbf{A}(\mathbf{r}) = A_x(\mathbf{r})\hat{\mathbf{x}} + A_y(\mathbf{r})\hat{\mathbf{y}} + A_z(\mathbf{r})\hat{\mathbf{z}}$. We use $\int dv = \int dxdydz$ for the integration over 3D space. We work in SI units.

II. REVIEW OF QUANTUM THEORY FOR SPONTANEOUS EMISSION

Spontaneous emission is an irreversible process whereby a quantum system makes a transition from an excited state to the ground state, while simultaneously emitting a photon into the vacuum. The general consensus is that spontaneous emission cannot fully be described by any classical electromagnetic theory; almost by definition, a complete description of spontaneous emission requires quantization of the photon field. In this section, we review the Weisskopf–Wigner theory[26,27] of spontaneous emission, evaluating both the expectation value of the electric field and the emission intensity.

A. Power-Zienau-Woolley Hamiltonian

Before studying spontaneous emission in detail, one must choose a Hamiltonian and a gauge for QED calculations. We will work with the Power-Zienau-Woolley Hamiltonian[28–30] in the Coulomb gauge (so that $\mathbf{A}_\parallel = 0$ and $\mathbf{A} = \mathbf{A}_\perp$) because we believe the method naturally offers a semiclassical interpretation:

$$\widehat{H}_{\mathrm{PZW}} = \widehat{H}_s + \widehat{H}_R + \widehat{H}_{\mathrm{int}}, \tag{1}$$

where

$$\widehat{H}_R = \int \mathrm{d}v \left\{ \frac{1}{2\epsilon_0}\widehat{\mathbf{D}}_\perp(\mathbf{r})^2 + \frac{1}{2\mu_0}\left(\nabla \times \widehat{\mathbf{A}}(\mathbf{r})\right)^2 \right\}, \tag{2}$$

$$\widehat{H}_{\mathrm{int}} = -\frac{1}{\epsilon_0}\int \mathrm{d}v \widehat{\mathbf{D}}_\perp(\mathbf{r}) \cdot \widehat{\mathbf{P}}_\perp(\mathbf{r}) + \frac{1}{2\epsilon_0}\int \mathrm{d}v \left|\widehat{\mathbf{P}}_\perp(\mathbf{r})\right|^2. \tag{3}$$

Here $\widehat{\mathbf{A}}(\mathbf{r})$ is the vector potential of the EM field and $\widehat{\mathbf{D}}_\perp(\mathbf{r})$ is the transverse field displacement, $\widehat{\mathbf{D}}_\perp(\mathbf{r}) = \epsilon_0\widehat{\mathbf{E}}_\perp(\mathbf{r}) + \widehat{\mathbf{P}}_\perp(\mathbf{r})$. $\widehat{H}_s$ is the Hamiltonian of the matter system and will be specified below. Note that the Power-Zienau-Woolley Hamiltonian is rigorously equivalent to the more standard $\widehat{\mathbf{P}} \cdot \widehat{\mathbf{A}}$ description of QED, but the matter field is now conveniently decomposed into a multipolar form. That being said, in Eq. (1) we have ignored the multipolar magnetization coupling; we are also assuming we may ignore any relativistic dynamics of the matter field.

For QED in the Coulomb gauge, the operator associated with the vector potential can be written in the formalism of second quantization:

$$\widehat{\mathbf{A}}(\mathbf{r}) = i\sum_{\mathbf{k}} \frac{\mathcal{E}_{\mathbf{k}}}{\omega_{\mathbf{k}}}\mathbf{e}_{\mathbf{k}}\left(\widehat{a}_{\mathbf{k}}e^{i\mathbf{k}\cdot\mathbf{r}} + \widehat{a}^\dagger_{\mathbf{k}}e^{-i\mathbf{k}\cdot\mathbf{r}}\right) \tag{4}$$

where the matrix element $\mathcal{E}_{\mathbf{k}} = \sqrt{\frac{\hbar\omega_{\mathbf{k}}}{2\epsilon_0 L^n}}$ is associated with the frequency $\omega_{\mathbf{k}} = c|\mathbf{k}|$, and L^n is the volume of the n-dimensonal space. $\widehat{a}_{\mathbf{k}}$ and $\widehat{a}^\dagger_{\mathbf{k}}$ are the destruction and creation operators of the photon field and satisfy the commutation relations: $\left[\widehat{a}_{\mathbf{k}}, \widehat{a}^\dagger_{\mathbf{k}'}\right] = \delta(\mathbf{k}-\mathbf{k}')$. The electric and magnetic fields can be obtained according to

$$\begin{aligned}\widehat{\mathbf{B}}(\mathbf{r}) &= \boldsymbol{\nabla} \times \widehat{\mathbf{A}}(\mathbf{r}) \\ &= i\sum_{\mathbf{k}} \mathcal{E}_{\mathbf{k}} \frac{\mathbf{k}\times\mathbf{e}_{\mathbf{k}}}{c}\left(\widehat{a}_{\mathbf{k}}e^{i\mathbf{k}\cdot\mathbf{r}} - \widehat{a}^\dagger_{\mathbf{k}}e^{-i\mathbf{k}\cdot\mathbf{r}}\right),\end{aligned} \tag{5}$$

$$\begin{aligned}\widehat{\mathbf{E}}_\perp(\mathbf{r}) &= -\frac{1}{c}\frac{\partial}{\partial t}\widehat{\mathbf{A}}(\mathbf{r}) \\ &= i\sum_{\mathbf{k}} \mathcal{E}_{\mathbf{k}}\mathbf{e}_{\mathbf{k}}\left(\widehat{a}_{\mathbf{k}}e^{i\mathbf{k}\cdot\mathbf{r}} - \widehat{a}^\dagger_{\mathbf{k}}e^{-i\mathbf{k}\cdot\mathbf{r}}\right),\end{aligned} \tag{6}$$

recalling that $\boldsymbol{\nabla}\cdot\widehat{\mathbf{A}}(\mathbf{r}) = 0$ in the Coulomb gauge. In term of $\widehat{\mathbf{E}}_\perp$ and $\widehat{\mathbf{B}}$, the transverse Hamiltonian of the EM field can be represented equivalently as

$$\begin{aligned}\widehat{H}_R &= \int \mathrm{d}v \left\{ \frac{\epsilon_0}{2}\widehat{\mathbf{E}}_\perp(\mathbf{r})^2 + \frac{1}{2\mu_0}\widehat{\mathbf{B}}(\mathbf{r})^2 \right\} \\ &= \sum_{\mathbf{k}} \hbar\omega_{\mathbf{k}}\left(\widehat{a}^\dagger_{\mathbf{k}}\widehat{a}_{\mathbf{k}} + \frac{1}{2}\right).\end{aligned} \tag{7}$$

As mentioned above, Eq. (1) has several advantages as a starting point for semiclassical QED. First, the electron–photon coupling is expressed in terms of the electric field and polarization, instead of vector potentials. In fact, the electric dipole Hamiltonian emerges easily if one further makes the long-wavelength approximation.[30] Second, according to Eq. (1), the displacement $\widehat{\mathbf{D}}_\perp(\mathbf{r})$ is effectively the momentum conjugate to the vector potential $\widehat{\mathbf{A}}(\mathbf{r})$, satisfying the canonical commutation relation, $[\widehat{\mathbf{D}}_\perp(\mathbf{r}), \widehat{\mathbf{A}}(\mathbf{r}')] = i\hbar\delta^\perp(\mathbf{r}-\mathbf{r}')$. This correspondence will allow us below to use a classical interpretation for propagating the classical EM field.

B. Electric Dipole Hamiltonian

In practice, for atomic problems we often consider an electronic system with a spatial distribution on the order of a Bohr radius interacting with an EM field which has a wavelength much larger than the size of the system. In this case, we can exploit the long-wavelength approximation and recover the standard electric dipole Hamiltonian (i.e. a generalized Göppert-Mayer transformation[30]):

$$\widehat{H}_{\text{int}} \approx -\widehat{\mathbf{d}} \cdot \widehat{\mathbf{E}}_{\perp} (\mathbf{r} = 0) . \tag{8}$$

In this representation, the coupling between the atom and the photon field is simple: one multiplies the dipole moment operator, $\widehat{\mathbf{d}} = \sum_{\alpha} q_{\alpha} \widehat{\mathbf{r}}_{\alpha}$, by the electric field evaluated at the origin (where the atom is positioned). This bi-linear electric dipole Hamiltonian is the usual starting point for studying quantum optical effects, such as spontaneous emission.

C. Quantum Theory of Spontaneous Emission

For a quantum electrodynamics description of spontaneous emission, we need to consider only a simple two-level system

$$\widehat{H}_s = \varepsilon_0 |0\rangle \langle 0| + \varepsilon_1 |1\rangle \langle 1| \tag{9}$$

which is coupled to the photon field. We assume $\varepsilon_0 < \varepsilon_1$ and $\varepsilon_1 - \varepsilon_0 = \hbar\Omega$. The electronic dipole moment operator takes the form of

$$\widehat{\mathbf{d}} = \boldsymbol{\mu}_{01} (|0\rangle \langle 1| + |1\rangle \langle 0|) , \tag{10}$$

where $\boldsymbol{\mu}_{01} = \langle 0| \sum_{\alpha} q_{\alpha} \widehat{\mathbf{r}}_{\alpha} |1\rangle$ is the transition dipole moment of the two states. Using Eq. (6), with a dipolar approximation, the coupling between the two level system and the photon field can be expressed as

$$-\widehat{\mathbf{d}} \cdot \widehat{\mathbf{E}}_{\perp} (\mathbf{r} = 0) = \sum_{\mathbf{k}} V_{\mathbf{k}} \left(\widehat{a}_{\mathbf{k}} - \widehat{a}_{\mathbf{k}}^{\dagger} \right) (|0\rangle \langle 1| + |1\rangle \langle 0|) \tag{11}$$

where the matrix element is given by $V_{\mathbf{k}} = i\mathcal{E}_{\mathbf{k}} \mathbf{e}_{\mathbf{k}} \cdot \boldsymbol{\mu}_{01}$. We assume the initial wavefunction is $|\psi (0)\rangle = c_0 (0) |0\rangle + c_1 (0) |1\rangle$ and the density matrix is $\rho_{ij} (0) = c_i (0) c_j^* (0)$.

Based on the generalization of Weisskopf–Wigner theory (see Appendix A), we can write down the excited state population as

$$\rho_{11} (t) = \rho_{11} (0) e^{-\kappa t} \tag{12}$$

in a coarse-grained sense (meaning that we average over a time scale τ satisfyting $2\pi/\Omega \ll \tau \ll 1/\kappa$). The decay rate for a three-dimensional system is given by the Fermi's golden rule (FGR) rate[31]

$$\kappa^{3\text{D}} = \frac{|\boldsymbol{\mu}_{01}|^2 \Omega^3}{3\pi\hbar\epsilon_0 c^3} . \tag{13}$$

Similarly, for an effectively one-dimensional system, we imagine a uniform charge distributions in the yz plane and a delta function in the x direction. The effective dipole moment in 1D is defined as $\mu_{01}^2 = |\boldsymbol{\mu}_{01}|^2 / L_y L_z$. The decay rate for this effectively 1D case is

$$\kappa^{1\text{D}} = \frac{\mu_{01}^2 \Omega}{\hbar\epsilon_0 c} . \tag{14}$$

Eqs (13) and (14) are proven in Ref 23, as well as in Appendix A. Below, we will use κ to represent the FGR rate for either $\kappa^{3\text{D}}$ or $\kappa^{1\text{D}}$ depending on context. Note that, in general, Fermi's golden rule is valid in the weak coupling limit ($\kappa \ll \Omega$), which is also called the FGR regime.

We assume that the initial condition of the photon field is a vacuum, i.e. there are no photon at $t = 0$. For a given initial state, $|\psi (0)\rangle = c_0 (0) |0\rangle + c_1 (0) |1\rangle$, the expectation value of the observed electric field for an effectively 1D system is given by

$$\langle \mathbf{E}_{\perp} (x, t) \rangle = |c_0 (t)| \, c_1 (0) \times R (x, t) \sin \Omega (t - |x| / c) \tag{15}$$

where

$$R (x, t) = \frac{\Omega \mu_{01}}{c\epsilon_0} e^{-\frac{\kappa}{2}\left(t - \frac{|x|}{c}\right)} \times \theta (ct - |x|) \tag{16}$$

Note that $R (x, t)$ contains an event horizon ($|x| < ct$) for the emitting radiation. The observed electric field represent the *coherent emission* at the frequency Ω. In a coarse-grained sense, since $\overline{\sin^2 \Omega t} \approx \frac{1}{2}$, the coherent emission has a magnitude given by

$$\overline{\langle \mathbf{E}_{\perp} (x, t) \rangle^2} = |c_0 (t)|^2 |c_1 (0)|^2 \times \frac{R (x, t)^2}{2} . \tag{17}$$

We note that the coherent emission depends on the instantaneous population of the ground state $|c_0 (t)|^2$.

The expectation value of the intensity distribution can be obtained as

$$\overline{\langle \mathbf{E}_{\perp}^2 (x, t) \rangle} = |c_1 (0)|^2 \times \frac{R (x, t)^2}{2} , \tag{18}$$

which conserves energy of the total system. Note that the variance of the observed electric field (i.e. the fact that $\overline{\langle \mathbf{E}_{\perp}^2 \rangle} \neq \overline{\langle \mathbf{E}_{\perp} \rangle^2}$) reflects a quantum mechanical feature of spontaneous emission. For proofs of Eqs. (15–18), see Appendix A.

III. EHRENFEST DYNAMICS AS ANSTAZ FOR QUANTUM ELECTRODYNAMICS

Ehrenfest dynamics provides a semiclassical anstaz for modeling QED based on a mean-field approximation together with a classical EM field and quantum matter field.[23] In general, a mean-field approximation is valid when the system does not have strong correlations among the subsystems.[22] In this section, we review the Ehrenfest approach for treating coupled electron–radiation dynamics, specifically spontaneous emission.

A. Semiclassical Hamiltonian

According to Ehrenfest dynamics, we define a semiclassical Hamiltonian, $\widehat{H}_{\rm SC}$ that approximates Eq. (1):[32]

$$\begin{aligned}\widehat{H}_{\rm SC} =&\widehat{H}_s - \int \mathrm{d}v \mathbf{E}_\perp(\mathbf{r},t)\,\widehat{\mathbf{P}}(\mathbf{r}) \\ &+ \int \mathrm{d}v \left\{ \frac{\epsilon_0}{2}\mathbf{E}_\perp(\mathbf{r},t)^2 + \frac{1}{2\mu_0}\mathbf{B}(\mathbf{r},t)^2 \right\}.\end{aligned} \tag{19}$$

Here, we treat the EM field operators as classical electrodynamics parameters $\widehat{\mathbf{D}} \to \mathbf{D}(\mathbf{r},t) = \epsilon_0\mathbf{E}_\perp(\mathbf{r},t) + \mathbf{P}_\perp(\mathbf{r},t)$ and $\nabla\times\widehat{\mathbf{A}} \to \mathbf{B}(\mathbf{r},t)$, so that we can commute $\mathbf{E}_\perp$ with $\widehat{\mathbf{P}}$ in the coupling term. Note that the average polarization is defined as $\mathbf{P}(\mathbf{r},t) = \mathrm{Tr}_s\left\{\widehat{\rho}(t)\,\widehat{\mathbf{P}}(\mathbf{r})\right\}$. From the semiclassical Hamiltonian, we can extract an electronic Hamiltonian

$$\widehat{H}^{\rm el} = \widehat{H}_s - \int \mathrm{d}v \mathbf{E}_\perp(\mathbf{r},t)\cdot\widehat{\mathbf{P}}(\mathbf{r}). \tag{20}$$

which depends only parametrically on the EM field.

B. Ehrenfest dynamics

Within Ehrenfest dynamics, the electronic system is described by the electronic density matrix $\widehat{\rho}(t)$ while the EM field, $\mathbf{E}(\mathbf{r},t)$ and $\mathbf{B}(\mathbf{r},t)$, are propagated by classical electrodynamics. The electronic density matrix evolves according to the Liouville equation,

$$\frac{\partial}{\partial t}\widehat{\rho}(t) = -\frac{i}{\hbar}\left[\widehat{H}^{\rm el}(\mathbf{E}),\widehat{\rho}(t)\right]. \tag{21}$$

The EM field is governed by Maxwell's equation for classical electrodynamics

$$\frac{\partial}{\partial t}\mathbf{B}(\mathbf{r},t) = -\boldsymbol{\nabla}\times\mathbf{E}_\perp(\mathbf{r},t), \tag{22}$$

$$\frac{\partial}{\partial t}\mathbf{E}_\perp(\mathbf{r},t) = c^2\boldsymbol{\nabla}\times\mathbf{B}(\mathbf{r},t) - \frac{1}{\epsilon_0}\mathbf{J}(\mathbf{r},t), \tag{23}$$

where the average current is generated by the average polarization of the electronic system

$$\mathbf{J}(\mathbf{r},t) = \frac{\partial}{\partial t}\mathrm{Tr}_s\left\{\widehat{\rho}(t)\,\widehat{\mathbf{P}}(\mathbf{r})\right\}. \tag{24}$$

The total energy of the electronic system and the classical EM field is

$$\begin{aligned}U_{\rm tot}(\widehat{\rho},\mathbf{E},\mathbf{B}) = &\mathrm{Tr}_s\left(\widehat{\rho}(t)\,\widehat{H}_s\right) + \\ &\int \mathrm{d}v\left(\frac{\epsilon_0}{2}\mathbf{E}_\perp(\mathbf{r},t)^2 + \frac{1}{2\mu_0}\mathbf{B}(\mathbf{r},t)^2\right).\end{aligned} \tag{25}$$

One of most important strengths is that the total energy is conserved (as can be shown easily). Altogether, Ehrenfest dynamics is a self-consistent, computationally inexpensive approach for propagating the electronic and EM field dynamics simultaneously.

C. Drawback of Ehrenfest Dynamics: Spontaneous Emission

For the purposes of this paper, it will now be fruitful to discuss spontaneous emission in more detail within the context of Ehrenfest dynamics. In the FGR regime, if we approximate the transition dipole moment of the two level system to be a delta function at the origin, we can show that the electric dipole coupling within Ehrenfest dynamics satisfies the relationship

$$H_{01}^{\rm el} = -\hbar\kappa\mathrm{Im}\rho_{01} \tag{26}$$

for both 1D and 3D systems. For a 1D system, this relation was derived previously in Ref. 23. For a 3D system, this relation can be derived using Jefimenko's equation of classical electrodynamics with a current source given by Eq. (24) (see Appendix B).

With Eq. (26), we can convert Liouville equation (Eq. (21)) of Ehrenfest dynamics into self-dependent, non-linear equations of motion

$$\frac{\partial\rho_{11}}{\partial t} = -2\kappa\left(\mathrm{Im}\rho_{01}\right)^2, \tag{27}$$

$$\frac{\partial\rho_{01}}{\partial t} = i\Omega\rho_{01} - i\kappa\mathrm{Im}\rho_{01}\left(\rho_{11}-\rho_{00}\right). \tag{28}$$

In the FGR regime, because $\kappa \ll \Omega$, we can approximate the coherence $\rho_{01} \approx \sqrt{\rho_{00}\rho_{11}}e^{i\Omega t}$ for a time τ satisfying $2\pi/\Omega \ll \tau \ll 1/\kappa$ so that $\left(\mathrm{Im}\rho_{01}\right)^2 \approx \rho_{00}\rho_{11}\sin^2\Omega t$. We may then define an instantaneous decay rate $k_{Eh}(t)$ for ρ_{11}, satisfying $\frac{\partial\rho_{11}}{\partial t} = -k_{Eh}(t)\,\rho_{11}$, where

$$k_{Eh}(t) = 2\kappa\rho_{00}(t)\sin^2\Omega t. \tag{29}$$

Note that ρ_{11} does not change much within the time scale τ. To see the population decay in a coarse-grain sense, let us perform a moving average over τ and denote the average decay rate as

$$\overline{k_{Eh}}(t) = \frac{1}{\tau}\int_t^{t+\tau} dt' k_{Eh}(t) = \kappa\rho_{00}(t); \tag{30}$$

here we have used $\overline{\sin^2\Omega t} \approx \frac{1}{2}$.

This analysis reveals the underlying detail of the Ehrenfest failure to capture spontaneous emission: Eq. (30) suggest that Ehrenfest dynamics actually yields a non-exponential decay and, when $\rho_{00} = 0$, Ehrenfest dynamics does not predict any spontaneous emission. More importantly, we find that the Ehrenfest decay rate as a function of t can be expressed as the correct spontaneous emission rate, only multiplied by the lower state population at time t.

IV. EHRENFEST+R METHOD

Given the failure of Ehrenfest dynamics to capture spontaneous emission fully as described above, we now propose an *ad hoc Ehrenfest+R* method for ensuring

that the dynamics of quantum subsystem in vacuum do agree with FGR decay. Our approach is straightforward: we will enforce an additional relaxation pathway on top of Ehrenfest dynamics such that the total Ehrenfest+R emission should agree with the true spontaneous decay rate. We will benchmark this Ehrenfest+R approach in the context of a two-level system in 1D or 3D space. Note that the classical radiation field is at zero temperature, so we may exclude all thermal transitions from $|0\rangle$ to $|1\rangle$. We begin by motivating our choice of an *ad hoc* algorithm. In Sec. IV C, we provide a flowchart so that the reader can easily reproduce our algorithm and data.

A. The Quantum Subsystem

1. Liouville equation

As far as the quantum subsystem is concerned, in order to recover the FGR rate of the population in the excited state, we will include an additional relaxation ("+R") term on top of the Liouville equation,

$$\frac{\partial \widehat{\rho}}{\partial t} = -\frac{i}{\hbar}\left[\widehat{H}^{\mathrm{el}}, \widehat{\rho}\right] + \mathcal{L}_R \widehat{\rho}, \tag{31}$$

where the super-operator $\mathcal{L}_R$ enforces relaxation. For a two-level system, the diagonal elements of the super-operator are chosen to be

$$\left[\mathcal{L}_R \widehat{\rho}\right]_{11} = -\left[\mathcal{L}_R \widehat{\rho}\right]_{00} = -k_R \rho_{11}, \tag{32}$$

and the the off-diagonal elements are determined by conserving the purity of the density matrix.[33]

The +R relaxation rate in Eq. (32) is chosen as

$$k_R \equiv 2\kappa \left(1-\rho_{00}\right) \mathrm{Im}\left[\frac{\rho_{01}}{|\rho_{01}|} e^{i\phi}\right]^2, \tag{33}$$

where κ is the FGR rate. Eq. (33) is similar to Eq. (29) but with an arbitrary phase $\phi \in (0, 2\pi)$. Averaging over a time scale τ (defined in Eq. (30)), we find

$$\overline{k_R} = \kappa\left(1-\rho_{00}\right). \tag{34}$$

Thus, the average total decay rate predicted by Eq. (31) is

$$\kappa = \overline{k_{Eh}} + \overline{k_R}. \tag{35}$$

In other words, Eqs. (31–33) should recover the true FGR rate and correct Ehrenfest dynamics.

The phase ϕ in Eq. (33) can be chosen arbitrarily without affecting the total decay rate in a coarse-grained sense (i.e. if we perform a moving average over τ). In what follows, we will run multiple trajectories (indexed by $\ell \in N_{\mathrm{traj}}$) with ϕ^ℓ chosen randomly. The choice of a random ϕ^ℓ allows us effectively to introduce decoherence on top of the average EM field, so that we may represent the time/phase uncertainty of the emitted light as an ensemble of classical fields. Each individual trajectory still concurrently carries a pure electronic wavefunction. Note that a random phase does not affect the FGR decay rate of the quantum subsystem.

2. Practical Implementation

In practice, we will work below with the wavefunction $|\psi\rangle$, rather than the density matrix $\widehat{\rho} = |\psi\rangle\langle\psi|$. For each time step dt, the wavefunction is evolved with a two-step propagation scheme:

$$|\psi(t+dt)\rangle = \widehat{\mathcal{T}}_{0\leftarrow 1}\left[k_R\right] \cdot e^{-i\widehat{H}^{\mathrm{el}}dt/\hbar} |\psi(t)\rangle. \tag{36}$$

The operator $e^{-i\widehat{H}^{\mathrm{el}}dt/\hbar}$ carries out standard propagation of the Schrödinger equation with the electronic Hamiltonian given by Eq. (20). The quantum transition operator $\widehat{\mathcal{T}}_{0\leftarrow 1}(k_R)$ implements the additional +R population relaxation from Eqs. (32) and (33). Explicitly, the transition operator is defined by

$$\begin{pmatrix} c_0' \\ c_1' \end{pmatrix} = \widehat{\mathcal{T}}_{0\leftarrow 1}\left[k_R\right] \begin{pmatrix} c_0 \\ c_1 \end{pmatrix} \tag{37}$$

where

$$c_1' = c_1 e^{-k_R dt/2} \approx \frac{c_1}{|c_1|}\sqrt{|c_1|^2 - k_R |c_1|^2\, dt}, \tag{38}$$

and if $|c_0| \neq 0$,

$$\begin{aligned} c_0' &= c_0\sqrt{1 + \frac{|c_1|^2}{|c_0|^2}\left(1-e^{-k_R dt}\right)} \\ &\approx \frac{c_0}{|c_0|}\sqrt{|c_0|^2 + k_R |c_1|^2\, dt} \end{aligned} \tag{39}$$

Note that the phase of the wavefunction is preserved by the transition operator in our implementation. In other words, the transition operator simply transfers $k_R |c_1|^2\, dt$ of population from $|1\rangle$ to $|0\rangle$ without changing the phase of the wavefunction.

Note that, if the subsystem happens to begin purely on the excited state (i.e. $\widehat{\rho} = |1\rangle\langle 1|$ or $|c_0| = 0$), there is an undetermined phase in the wavefunction representation. In other words, we can write say $|\psi\rangle = e^{i\theta}|1\rangle$ and choose θ randomly. In this case, the transition operator is defined as

$$c_1' = e^{i\theta} e^{-\kappa dt/2} \approx e^{i\theta}\sqrt{1-\kappa dt}, \tag{40}$$

$$c_0' = \sqrt{1-e^{-\kappa dt}} \approx \sqrt{\kappa dt}. \tag{41}$$

As emphasized in Ref. 23 and Sec. III, for these initial conditions, $\overline{k_{Eh}} = 0$ and $\overline{k_R} = \kappa$ so that the +R relaxation must account for all of the required spontaneous decay.

3. Energy Conservation

While Ehrenfest dynamics conserves the total energy of the quantum subsystem together with the EM field, our proposed extra +R relaxation changes the energy of the quantum subsystem by an additional amount:

$$\frac{dU_s}{dt} = \mathrm{Tr}\left\{\widehat{H}_s \mathcal{L}_R \widehat{\rho}\right\} = -\Omega k_R \rho_{11}. \tag{42}$$

Thus, during a time step dt, the change in energy for the radiation field is

$$\delta U_R = \Omega k_R \rho_{11} dt. \tag{43}$$

For the Ehrenfest+R approach to enforce the energy conservation, this energy loss must flow into the EM field in the form of light emission. In other words, we must rescale the $\mathbf{E}$ and $\mathbf{B}$ fields.

B. The Classical EM fields

At every time step, with the +R correction of the quantum wavefunction, we will rescale the Ehrenfest EM field ($\mathbf{E}_{Eh}$ and $\mathbf{B}_{Eh}$) for each trajectory (ℓ) as follows:

$$\mathbf{E}^{\ell}_{Eh+R} = \mathbf{E}^{\ell}_{Eh} + \alpha^{\ell} \delta \mathbf{E}_R, \tag{44}$$

$$\mathbf{B}^{\ell}_{Eh+R} = \mathbf{B}^{\ell}_{Eh} + \beta^{\ell} \delta \mathbf{B}_R, \tag{45}$$

or, in matrix notation,

$$\begin{pmatrix} \mathbf{E}^{\ell}_{Eh+R} \\ \mathbf{B}^{\ell}_{Eh+R} \end{pmatrix} = \mathcal{R}\left[\delta U^{\ell}_R\right] \begin{pmatrix} \mathbf{E}^{\ell}_{Eh} \\ \mathbf{B}^{\ell}_{Eh} \end{pmatrix}. \tag{46}$$

Here, the coefficients α^{ℓ} and β^{ℓ} depend on the random phase ϕ^{ℓ} from Sec. IV A. In choosing the rescaling function $\mathcal{R}\left[\delta U^{\ell}_R\right]$, there are several requirements:

(a) $\delta \mathbf{E}_R$ and $\delta \mathbf{B}_R$ must be transverse fields.

(b) Since the +R correction enforces the FGR rate, it is crucial that the rescaled EM field does not interfere with propagating the quantum subsystem. Therefore, the spatial distribution of $\delta \mathbf{E}_R$ and $\delta \mathbf{B}_R$ must be located outside of the polarization distribution, such that $\int \mathrm{d}v \widehat{\mathbf{P}} \cdot \delta \mathbf{E}_R \approx 0$, ensuring the electronic Hamiltonian, Eq. (20), does not change much after we rescale the classical EM field.

(c) The magnitude of $\beta \delta \mathbf{B}_R$ must be equal to $1/c$ times the magnitude of $\alpha \delta \mathbf{E}_R$ for all $\mathbf{r}$ in space so that the emission light propagates only in one direction.

(d) The directional energy flow must be outward, i.e. the Poynting vector, $\mathbf{S} = \frac{1}{\mu_0} \mathbf{E}_{Eh+R} \times \mathbf{B}_{Eh+R}$ must have $\mathbf{S}(\mathbf{r}) \cdot \hat{\mathbf{r}} > 0$ for all $\mathbf{r}$ (assuming the light is emanating from the origin).

(e) On average, we must have energy conservation, i.e. the energy increase of the classical EM field must be equal to the energy loss of the quantum subsystem described in Eq. (43).

Unfortunately, it is very difficult to satisfy all of these requirements concurrently, especially (c), (d), and (e). Nevertheless, we will make an anstaz below which we believe will be robust.

Given a polarization distribution $\mathbf{P}$, the rescaling functions for our anstaz are chosen to be of the form

$$\delta \mathbf{E}_R = \boldsymbol{\nabla} \times \boldsymbol{\nabla} \times \mathbf{P} - g \mathbf{P}_{\perp}, \tag{47}$$

$$\delta \mathbf{B}_R = \boldsymbol{\nabla} \times \mathbf{P} - h \left(\boldsymbol{\nabla} \times\right)^3 \mathbf{P}, \tag{48}$$

where g and h are chosen best accommodate requirements (b)–(d). Note that Eqs. (47) and (48) are both transverse fields. The rescaling anstaz in Eq. (47) and (48) are motivated by a comparison of the electrodynamical quantum–classical Liouville equation (QCLE) and Ehrenfest dynamics in the framework of mixed quantum-classical theory (to be published). In 3D space, we simply choose $g = h = 0$, but dynamics in 1D are more complicated. In Appendix C, we show numerically that $\boldsymbol{\nabla} \times \boldsymbol{\nabla} \times \mathbf{P}$ and $\boldsymbol{\nabla} \times \mathbf{P}$ are good directions of the emanated $\mathbf{E}$ and $\mathbf{B}$ fields in 3D. For a 1D geometry, one prescription to choose g and h is to minimize the spatial overlap of both $\delta \mathbf{E}_R \cdot \mathbf{P}$ and $\delta \mathbf{B}_R \cdot \mathbf{P}$ (also see Appendix C).

For a Ehrenfest+R trajectory (labeled by ℓ), the parameters α^{ℓ} and β^{ℓ} are chosen to be

$$\alpha^{\ell} = \sqrt{\frac{cdt}{\Lambda} \frac{\delta U^{\ell}_R}{\epsilon_0 \int \mathrm{d}v \left|\delta \mathbf{E}_R\right|^2}} \times \mathrm{sgn}\left(\mathrm{Im}\left[\rho_{01} e^{i\phi^{\ell}}\right]\right) \tag{49}$$

$$\beta^{\ell} = \sqrt{\frac{cdt}{\Lambda} \frac{\mu_0 \delta U^{\ell}_R}{\int \mathrm{d}v \left|\delta \mathbf{B}_R\right|^2}} \times \mathrm{sgn}\left(\mathrm{Im}\left[\rho_{01} e^{i\phi^{\ell}}\right]\right) \tag{50}$$

where Λ is self-interference length determined by Eqs. (D8–D9). Note that Λ is associated with the spatial geometry of $\boldsymbol{\nabla} \times \boldsymbol{\nabla} \times \mathbf{P}$ and $\boldsymbol{\nabla} \times \mathbf{P}$. For $\mathbf{P}$ in the form of a Gaussian distribution (e.g. e^{-ax^2} in a 1D system), we find that the self-interference length is always $\Lambda^{1\mathrm{D}} = 2.363/\sqrt{2a}$. By construction, Eqs. (49) and (50) should conserve energy only on average, i.e. an individual trajectory with a random phase ϕ^{ℓ} may not conserve energy, but the ensemble energy should satisfy energy conservation (see Appendix D).

C. Step-by-step Algorithm of Ehrenfest+R method

Here we give a detailed step-by-step outline of the Ehrenfest+R method. For now, we restrict ourselves to the case of two electronic states. Given a polarization $\mathbf{P}(\mathbf{r})$ between the electronic states, before starting an

Ehrenfest+R trajectory, we precompute the FGR rate κ (Eq. (13) or Eq. (14)) and a self-interference length Λ (see Appendix D). At this point, we can initialize an Ehrenfest+R trajectory ℓ with a random phase ϕ^ℓ. For time step dt,

1. Propagate the wavefunction by $|\psi_{Eh}(t+dt)\rangle = e^{-i\widehat{H}^{\rm el}dt/\hbar}|\psi(t)\rangle$ and the EM field by Maxwell equations, Eqs. (22) and (23). Here, we denote the EM field as $\mathbf{E}^\ell_{Eh}(t+dt)$ and $\mathbf{B}^\ell_{Eh}(t+dt)$ and $\widehat{H}^{\rm el}$ is defined by Eq. (20).

2. Calculate the complementary rate k^ℓ_R (Eq. (33)) and energy change δU^ℓ_R (Eq. (43)).

3. Apply the transition operator $|\psi(t+dt)\rangle = \widehat{\mathcal{T}}_{0\leftarrow 1}\left[k^\ell_R\right]|\psi_{Eh}(t+dt)\rangle$ by Eq. (37).

4. Calculate α^ℓ and β^ℓ according to Eq. (49) and Eq. (50) and then rescale the EM field by $\begin{pmatrix}\mathbf{E}^\ell(t+dt)\\ \mathbf{B}^\ell(t+dt)\end{pmatrix} = \mathcal{R}\left[\delta U^\ell_R\right]\begin{pmatrix}\mathbf{E}^\ell_{Eh}(t+dt)\\ \mathbf{B}^\ell_{Eh}(t+dt)\end{pmatrix}$ according to Eq. (44–46).

5. Apply absorbing boundary conditions if the classical EM field reaches the end of the spatial grid.

V. RESULTS: SPONTANEOUS EMISSION

As a test for our proposed Ehrenfest+R anstaz, we study spontaneous emission of a two-level system in vacuum for 1D and 3D systems. We assume the system lies in the FGR regime and the polarization distribution is relatively small in space so that the long-wavelength approximation is valid. For the two-level system with energy difference $\varepsilon_1 - \varepsilon_0 = \hbar\Omega$, we consider two types of initial conditions $|\psi(0)\rangle$ with distinct behaviors:

#1 A superposition state with a fixed relative phase, i.e. $|\psi(0)\rangle = c_0|0\rangle + c_1|1\rangle$ where $|c_0|^2 + |c_1|^2 = 1$ and $|c_0| \neq 0$, $|c_1| \neq 1$:

- The upper state population $\rho_{11}(t)$ should decay according to the FGR rate.
- According to Eqs. (15)–(18), the electric field $\langle\mathbf{E}\rangle$ should exhibit coherent emission at frequency Ω.
- The averaged intensity $\langle\mathbf{E}^2\rangle$ should not equal the coherent emission $\langle\mathbf{E}\rangle^2$, i.e. $\langle\mathbf{E}^2\rangle - \langle\mathbf{E}\rangle^2 \neq 0$.

#2 A pure state with a random phase, i.e. $\widehat{\rho}(0) = |1\rangle\langle 1|$, which corresponds to $|\psi(0)\rangle = e^{i\theta}|1\rangle$ where θ is a random phase:

- The upper state population $\rho_{11}(t)$ should still decay according to the FGR rate.
- The electric field of each individual trajectory should oscillate at frequency Ω, but the phases of different trajectories should cancel out—so that the ensemble average of the electric field becomes zero, i.e. $\langle\mathbf{E}\rangle = 0$.
- The averaged intensity should not vanish, i.e. $\langle\mathbf{E}^2\rangle \neq 0$.

Model problems #1 and #2 capture key features when simulating spontaneous emission and can be considered critical tests for the proposed Ehrenfest+R approach. The parameters for our simulation are as follows. The energy difference of the two levels system is $\hbar\Omega = 16.46$ eV. The transition dipole moment is $\mu_{01} = 11282$ C/nm/mol.

For a 1D geometry, we consider a polarization distribution of the form:

$$\mathbf{P}^{\rm 1D}(x) = \mu_{01}\sqrt{\frac{a}{\pi}}e^{-ax^2}\hat{\mathbf{z}}, \tag{51}$$

with $a = 1/2\sigma^2$ and $\sigma = 3.0$ nm. According to Eq. (51), the polarization is in the z direction varying along the x direction. For this polarization, the self-interference length is $\Lambda^{\rm 1D} \approx 7.0$ nm. We use the rescaling function derived in Appendix. C:

$$\delta\mathbf{E}^{\rm 1D}_R(x) = -\mu_{01}\sqrt{\frac{a}{\pi}}4a^2x^2e^{-ax^2}\hat{\mathbf{z}}, \tag{52}$$

$$\delta\mathbf{B}^{\rm 1D}_R(x) = \mu_{01}\sqrt{\frac{a}{\pi}}\frac{4}{3}a^2x^3e^{-ax^2}\hat{\mathbf{y}}. \tag{53}$$

For a 3D geometry, we again assume the polarization is only in the z direction, now of the form

$$\mathbf{P}^{\rm 3D}(\mathbf{r}) = \hat{\mathbf{z}}\mu_{01}\frac{2a^{3/2}}{\pi^{3/2}}e^{-ar^2}, \tag{54}$$

where we use the same parameters for a and μ_{01} as for the 1D geometry. The rescaling field in 3D is chosen to be:

$$\delta\mathbf{E}^{\rm 3D}_R(\mathbf{r}) = \boldsymbol{\nabla}\times\boldsymbol{\nabla}\times\mathbf{P}^{\rm 3D}(\mathbf{r}), \tag{55}$$

$$\delta\mathbf{B}^{\rm 3D}_R(\mathbf{r}) = \boldsymbol{\nabla}\times\mathbf{P}^{\rm 3D}(\mathbf{r}). \tag{56}$$

The self-interference length can be obtained numerically as $\Lambda^{\rm 3D} \approx 0.6$ nm.

Our simulation is propagated using Cartesian coordinates with $dx = 0.1$ for 1D and $dx = dy = dz = 0.1$ for 3D. The time step is $dt = 0.1$. Without loss of generality, the random phase ϕ^ℓ for Ehrenfest+R trajectories is chosen from an evenly space distribution, i.e. $\phi^\ell = 2\pi j/N_{\rm traj}$ for $j = 1, \cdots, N_{\rm traj}$.

A. Spontaneous decay rate

Our first focus is an initially coherent state with $\rho_{00}(0) = \rho_{11}(0) = 0.5$ above. We plot the upper state population and the decay rate of a 1D system in Fig 1(a). As shown in Ref. 23 and summarized in Sec. III above,

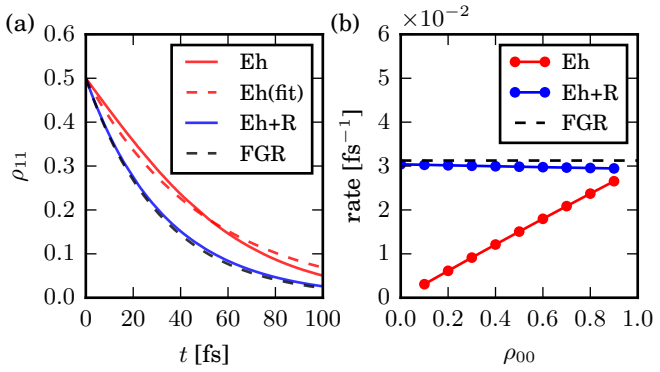

Figure 1. (a) Population of the excited state as a function of time. The initial state is $|\psi\rangle = \sqrt{\frac{1}{2}}|0\rangle + \sqrt{\frac{1}{2}}|1\rangle$. The black dash line indicate the FGR decay. The red solid line is the standard Ehrefest dynamics and the red dash line is an exponential fitting of the data. The blue solid line is Ehrefest+R dynamics with $N_{\text{traj}} = 40$. (b) Spontaneous decay rates extracted from excited state population dynamics for different initial states. As a function of the initial ground state population ρ_{00}, the exponential decay rates are obtained by the standard Ehrenfest method (red) and Ehrenfest+R method (blue). The black dash line indicate the FGR rate. Note that, for all cases, the Ehrenfest+R dynamics recover the true FGR spontaneous emission rate.

standard Ehrenfest dynamics does not agree with the FGR decay and cannot be fit to an exponential decay. With Ehrenfest+R dynamics, however, we can quantitatively correct the errors of Ehrenfest dynamics and recover the full spontaneous decay rate accurately. Furthermore, in Fig. 1(b) we prove that, even though Ehrenfest dynamics fails to predict the correct decay rate as a function of initial condition, the decay rate extracted from Ehrenfest+R dynamics agrees very well with the FGR decay rate for all initial conditions. Note that, for the extreme case $\rho_{00}(0) = 0$, Ehrenfest dynamics does not predict any population decay.

B. Emission Fields in 1D

We now turn our attention to the coherent emission and the intensity of the EM field. We start by considering the 1D geometry. According to Eq. (15), for a given time t, the electric field of spontaneous emission can be expressed as a function of x and shows oscillatory behavior of $\sin\Omega(t - |x|/c)$ for short time. Also, an event horizon is observed at $|x| = ct$, i.e. no electric field should be observed for $|x| > ct$ because of causality.

We find that the electric field obtained by an individual Ehrenfest+R trajectory shows the correct oscillations at frequency Ω with an additional phase shift. For an initially coherent state, the ensemble average of Ehrenfest+R trajectories agrees with Eq. (15) very well (see Figs. 2(a) and 2(b) for two cases with different initial conditions.) When the initial state is exclusively the excited state, the ensemble average of Ehrenfest+R trajectories vanishes by phase cancellation and we recover $\langle \mathbf{E} \rangle = 0$ (see Fig. 2(c)).

Now we compare the emission intensity $\overline{\langle \mathbf{E}^2 \rangle}$ and the magnitude of the coherent emission $\overline{\langle \mathbf{E} \rangle}^2$. On the right panels of Fig. 2, we plot the coarse-grained behavior of Ehrenfest+R trajectories. We show that Ehrenfest+R can accurately recover the spatial distribution of both $\overline{\langle \mathbf{E}^2 \rangle}$ and $\overline{\langle \mathbf{E} \rangle}^2$, as well as the event horizon. Note that in Fig. 2, the electric field and the intensity at large x corresponds to emission at earlier times. If we start with a coherent initial state, the relative proportion of coherent emission is given by $\overline{\langle \mathbf{E} \rangle}^2 / \overline{\langle \mathbf{E}^2 \rangle} = \rho_{00}\left(t - \frac{|x|}{c}\right)$, see Eqs. (15) and (17). For $\rho_{11}(0) = 0.5$, the coherent emission is responsible for 50% of the total energy emission at early times ($x \sim ct = 3 \times 10^4$ nm), and the coherent emission dominates later ($x \sim 0$). Obviously, if we begin with a wavefunction prepared exclusively on the excited state, there is no coherent emission due to phase cancellation among Ehrenfest+R trajectories. In the end, using an ensemble of trajectories with random phases ϕ^ℓ, Ehrenfest+R is effectively able to introduce some quantum decoherence among the classical trajectories and can recover both $\overline{\langle \mathbf{E}^2 \rangle}$ and $\overline{\langle \mathbf{E}^2 \rangle}$.

This behavior of Ehrenfest+R dynamics should be contrasted with the behavior of standard Ehrenfest dynamics, where we run only one trajectory and we observe only coherent emission with $\langle \mathbf{E}^2 \rangle = \langle \mathbf{E} \rangle^2$. Although the coherent emission obtained by standard Ehrenfest dynamics is close to the quantum result when $\rho_{11}(0)$ is small (see Fig. 2(a)), the magnitude of the coherent emission is incorrect in general. The electric field does oscillate at the correct frequency.

C. Emission Fields in 3D

For a 3D geometry, for reasons of computational cost, we propagate the dynamics of spontaneous emission for short-times only ($t < 1.0$ fs). Our results are similar to the 1D case and are plotted in Fig. 3. For a coherent initial state (Fig. 3 (a), (c)), each Ehrenfest+R trajectory yields an electric field and EM intensity oscillating at frequency Ω, and these features are retained by the ensemble average. For the case of dynamics initiated from the excited state only (Fig. 3 (b), (d)), each trajectory still oscillates at frequency Ω, but the average electric field is zero ($\langle \mathbf{E} \rangle = 0$) so that the peak of the spectrum vanishes.

In Fig. 3, we also compare our result versus the well-known classical Poynting flux of electric dipole radiation. In Fig. 3 (a), our reference is

$$I(\mathbf{r}, t) = \frac{\mu_0}{c^2} \frac{\Omega^4 \mu_{01}^2}{16\pi^2} \frac{\sin^2\theta}{r^2} \sin^2\Omega\left(t - \frac{r}{c}\right), \qquad (57)$$

and, in Fig. 3 (b), our reference is the mean electromag-

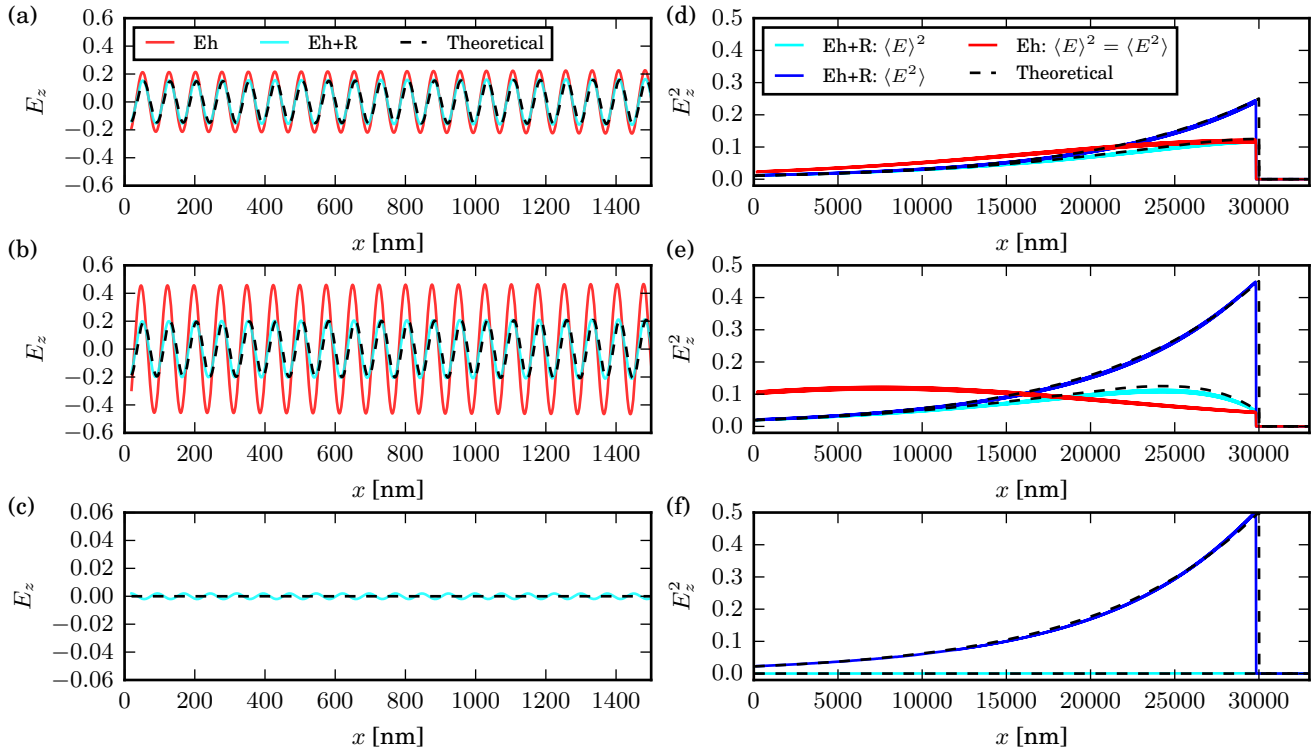

Figure 2. The electric field produced for spontaneous emission as a function of x at $t = 100$ fs. The initial population on the excited state is $\rho_{11}(0) = 0.5$ for (a), (d), $\rho_{11}(0) = 0.9$ for (b), (e), and $\rho_{11}(0) = 1$ for (c), (f). Left panels are the electric field in the z direction $\langle E_z\rangle$ in the unit of $\mu_{01}\Omega/\epsilon_0 c$, where the black dashed lines are the theoretical results (see Eq. (15).) The solid lines are calculated by standard Ehrenfest (red) and by Ehrenfest+R (cyan) dynamics. Right panels are the intensity ($\langle E_z^2\rangle$) and the magnitude of the coherent emission ($\langle E_z\rangle^2$) in the unit of $(\mu_{01}\Omega/\epsilon_0 c)^2$, where the black dashed lines are Eq. (17) and Eq. (18). On the right panels, we perform a moving average over $c\tau = 720$ nm (10 oscillations) to show the coarse-grained behavior. The solid lines are $\langle E_z^2\rangle = \langle E_z\rangle^2$ calculated by standard Ehrenfest dynamics (red), and $\langle E_z^2\rangle$ (blue) and $\langle E_z\rangle^2$ (cyan) calculated by Ehrenfest+R approach. The event horizon can be observed at $x = ct = 30000$ nm. $N_{\text{traj}} = 40$. Note that Ehrenfest+R covers all observables quantitatively, whereas Ehrenfest dynamics are accurate only when $\rho_{11}(0) \ll 1$. Note also that Ehrenfest dynamics predicts no emission when $\rho_{00}(0) = 0$ (f).

netic energy flux

$$\overline{I}(\mathbf{r}) = \frac{\mu_0}{c^2}\frac{\Omega^4\mu_{01}^2}{32\pi^2}\frac{\sin^2\theta}{r^2}. \tag{58}$$

In general, Ehrenfest+R dynamics yields a similar distribution as the classical dipole radiation. When initiated from a coherent state, both methods behave as $\sin^2\Omega\left(t-\frac{r}{c}\right)$; when initiated from a excited state, Ehrenfest+R method shows $1/r^2$ dependence while Ehrenfest dynamics does not yield any emission (not shown in the plot.) However, we note that the intensity of the Ehrenfest+R results is slightly larger than that of classical dipole radiation. This difference is attributed to the fact that the classical dipole radiation includes only coherent emission, which is captured by standard Ehrenfest dynamics. By contrast, Ehrenfest+R dynamics can also yield so-called incoherent emission ($\langle\mathbf{E}^2\rangle - \langle\mathbf{E}\rangle^2 \neq 0$), which is effectively a quantum mechanical feature with no classical analogue.

VI. CONCLUSIONS AND FUTURE WORKS

In this work, we have proposed a heuristic, new semi-classical approach to quantum electrodynamics, based on Ehrenfest dynamics and designed to capture spontaneous emission correctly. Our anstaz is to enforce extra electronic relaxation while also rescaling the EM field in the direction $\delta\mathbf{E}_R = \boldsymbol{\nabla}\times\boldsymbol{\nabla}\times\mathbf{P}$ and $\delta\mathbf{B}_R = \boldsymbol{\nabla}\times\mathbf{P}$. Our results suggest that this Ehrenfest+R approach can indeed recover the correct FGR decay rate for a two-level system. More importantly, both intensity and coherent emission can be accurately captured by Ehrenfest+R dynamics, where an ensemble of classical trajectories effectively simulates the statistical variations of a quantum electrodynamics field.

As far as computational cost is concerned, one Ehrenfest+R trajectory costs roughly the same amount as one standard Ehrenfest trajectory, and all dynamics are numerically stable. Implementation of Ehrenfest+R dynamics is easy to parallelize and incorporate within sophisticated numerical packages for classical electromag-

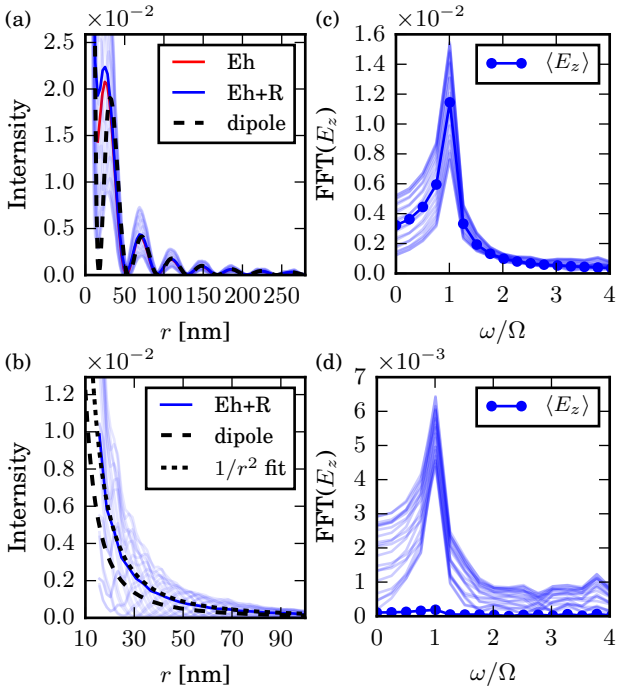

Figure 3. Spontaneous emission intensity calculated by Ehrenfest+R method as a function of radius r at $t = 1.0$ fs for the initial population (a) $\rho_{11} = 0.5$, and (b)$\rho_{11} = 1.0$. The polar angle is $\theta = \frac{\pi}{2}$ and the intensity is plotted in the unit of $\mu_0\Omega^4\mu_{01}^2/32\pi^2c^2$.The right panels are the corresponding spectrum of the electric field in the z direction. The dim lines are data from individual trajectories and the solid circles are the average data. The black dashed line is the theoretical energy flux. The self-interference length is $\Lambda^{3D} \approx 0.6$ nm.

netics (e.g. FDTD.)

Given the promising results presented above for Ehrenfest+R, we can foresee many interesting applications. First, we would like to include nuclear degrees of freedom within the quantum subsystem to explicitly address the role of dephasing in spontaneous and stimulated emission. Second, we would like to study more than two states. For instance, a three-level system with an incoming EM field can be employed for studying inelastic light scattering processes, such as Raman spectroscopy. Third, we would also like to model multiple spatial separated quantum emittors, such as resonance energy transfer.

At the same time, many questions remain and need to be addressed:

1. The current prescription for Ehrenfest+R approach is fundamentally based on enforcing the FGR rate. However, in many physical situations, such as molecules in a resonant cavity or near a metal surface, the decay rate of the quantum subsystem can be modified by interactions with environmental degrees of freedom. How should we modify the Ehrenfest+R approach to account for each environment?

2. For a quantum subsystem interacting with a strong incoming field, including the well-known Mollow triplet phenomenon and other multi-photon processes, EM field quantization can lead to complicated emission spectra involving frequencies best described with dressed states. Can these effectively quantum features be captured by Ehrenfest+R dynamics?

3. Finally, and most importantly, it remains to test how the approach presented here behaves when there are many quantum subsystems interacting, leading to coherent effects (i.e. plasmonic excitation). Can our approach simulate these fascinating experiments?

These questions will be investigated in the future.

ACKNOWLEDGMENT

This work is supported by AAA. We would like to thank BBB.

Appendix A: Generalized Weisskopf–Wigner Theory of Spontaneous Emission

Consider the electric dipole Hamiltonian given by Eq. (11). For comparison with semiclassical dynamics in Sec. V we will now derive the exact population dynamics and the emission EM field of a two level system in vacuum based on Weisskopf–Wigner theory and a retarded Green's function approach.

1. Dressed state representation

Let $|0, \cdots, 1_{\mathbf{k}}, \cdots, 0\rangle$ be a fock-space state of the EM field with one photon of mode $\omega_{\mathbf{k}}$. Let us denote the vacuum state as $|\{0\}\rangle$. For a system composed of an atom interacting with the EM field, the dressed state representation has the following basis (including up to single photon)[27,31]

$$|j;\mathbf{k}\rangle = |j\rangle\,|0, \cdots, 1_{\mathbf{k}}, \cdots, 0\rangle \tag{A1}$$
$$|j;0\rangle = |j\rangle\,|\{0\}\rangle \tag{A2}$$

Here $|j\rangle = |0\rangle, |1\rangle$ are the wavefunctions of the two level system. For such a system, the total wavefunction in the dressed state representation is therefore of the form:

$$\begin{aligned}|\psi(t)\rangle =& C_{0,0}(t)\,|0;0\rangle + C_{1,0}(t)\,|1;0\rangle + \\ & \sum_{\mathbf{k}} C_{0,\mathbf{k}}(t)\,|0;\mathbf{k}\rangle + \sum_{\mathbf{k}} C_{1,\mathbf{k}}(t)\,|1;\mathbf{k}\rangle\,.\end{aligned} \tag{A3}$$

Finally, for spontaneous emission, the initial wavefunction of the two-level system in vacuum is

$$|\psi(0)\rangle = C_0\,|0;0\rangle + C_1\,|1;0\rangle \tag{A4}$$

with $|C_0|^2+|C_1|^2=1$. We would like to propagate $|\psi(0)\rangle$ and calculate $|\psi(t)\rangle$ as a function of time. We emphasize that, in Eqs. (A3) and (A4), Hilbert space is restricted to one photon states.

For visualization purpose, it is helpful to write down the electric dipole Hamiltonian explicitly in matrix form in the dressed state representation,

$$\mathcal{H}=\mathcal{H}_0+\mathcal{V} \tag{A5}$$
$$=\begin{array}{c} \begin{matrix} \{|0;\mathbf{k}\rangle\} & |0;0\rangle & |1;0\rangle & \{|1;\mathbf{k}\rangle\} \end{matrix} \\ \begin{pmatrix} \{[\varepsilon_0+\hbar\omega_{\mathbf{k}}]\} & 0 & [\{V_{\mathbf{k}}\}]^\dagger & 0 \\ 0 & \varepsilon_0 & 0 & [\{V_{\mathbf{k}}\}] \\ [\{V_{\mathbf{k}}\}] & 0 & \varepsilon_1 & 0 \\ 0 & [\{V_{\mathbf{k}}\}]^\dagger & 0 & \{[\varepsilon_1+\hbar\omega_{\mathbf{k}}]\} \end{pmatrix} \end{array}$$

Here the set $\{[\varepsilon_j+\hbar\omega_{\mathbf{k}}]\}$ are an infinite set of matrices with exclusively diagonal elements $\varepsilon_j+\hbar\omega_{\mathbf{k}}$ for $j=0,1$. $[V_{\mathbf{k}}]$ is an infinite row with corresponding elements

$$V_{\mathbf{k}}=i\boldsymbol{\mu}_{01}\cdot\mathbf{e}_{\mathbf{k}}\sqrt{\frac{\hbar\omega_{\mathbf{k}}}{2\epsilon_0 L^n}} \tag{A6}$$

between the vacuum state $|\{0\}\rangle$ and one photon state of mode $\omega_{\mathbf{k}}$. Let us denote the diagonal part of the matrix as the unperturbed Hamiltonian $\mathcal{H}_0$ and the off-diagonal part as the coupling Hamilton $\mathcal{V}$. Note that the two quantum states in vacuum ($|0;0\rangle$ and $|1;0\rangle$) are coupled to two different continuous manifolds ($\{|1;\mathbf{k}\rangle\}$ and $\{|0;\mathbf{k}\rangle\}$), respectively.

Given that $\varepsilon_0<\varepsilon_1$, the $\{|0;\mathbf{k}\rangle\}$ manifold will always include a quantum state that is energetically resonant with the $|1;0\rangle$ state. However, the the $\{|1;\mathbf{k}\rangle\}$ manifold will always be off-resonant with $|0;0\rangle$ for all $\mathbf{k}$. Therefore, as the lowest order approximation, we can assume $C_{1,\mathbf{k}}(t)\approx 0$ and

$$C_{0,0}(t)\approx|C_{0,0}(t)|\,e^{-i\varepsilon_0 t/\hbar} \tag{A7}$$

for short time behavior.

2. Retarded Green's function formulation

We employ a retarded Green's function formulation[31] to obtain the time evolution of $C_{1,0}(t)$ and $C_{0,\mathbf{k}}(t)$. The retarded Green's operators are $\mathcal{G}(\varepsilon)=[\varepsilon-\mathcal{H}+i\eta]^{-1}$ for the full Hamiltonian and $\mathcal{G}_0(\varepsilon)=[\varepsilon-\mathcal{H}_0+i\eta]^{-1}$ for the unperturbed Hamiltonian where η is a positive small quantity ($\eta\to 0^+$). Using Dyson's identity $\mathcal{G}=\mathcal{G}_0+\mathcal{G}_0\mathcal{V}\mathcal{G}=\mathcal{G}_0+\mathcal{G}\mathcal{V}\mathcal{G}_0$, we can obtain the retarded Green's function in a self-consistent expression

$$\mathcal{G}_{11}(\varepsilon)=\frac{1}{\varepsilon-\varepsilon_1+i\eta+\frac{i}{2}\Gamma(\varepsilon)}, \tag{A8}$$
$$\mathcal{G}_{\mathbf{k}1}(\varepsilon)=\frac{V_{\mathbf{k}}}{\varepsilon-\varepsilon_0-\hbar\omega_{\mathbf{k}}+i\eta}\frac{1}{\varepsilon-\varepsilon_1+i\eta+\frac{i}{2}\Gamma(\varepsilon)} \tag{A9}$$

where the self energy is $\Gamma(\varepsilon)=2i\sum_{\mathbf{k}}|V_{\mathbf{k}}|^2/(\varepsilon-\varepsilon_0-\hbar\omega_{\mathbf{k}}+i\eta)$. The self energy can be evaluated by a Cauchy integral identity (ignoring the principle value part). For 1D, we can consider a dipole moment μ_{01} and use the density of states of a 1D system to obtain the self energy as

$$\begin{aligned}\Gamma^{1\mathrm{D}}(\varepsilon)&=2i\frac{L}{2\pi}\int dk\frac{\mu_{01}^2\mathcal{E}_k^2}{\varepsilon-\varepsilon_0-\hbar\omega_{\mathbf{k}}+i\eta}\\&=i\frac{\mu_{01}^2}{2\pi\epsilon_0\hbar c}\left[-i\pi(\varepsilon-\varepsilon_0)\right]\\&=\frac{\mu_{01}^2}{\epsilon_0\hbar c}(\varepsilon-\varepsilon_0)\end{aligned}$$

Here, $\mathcal{E}_{\mathbf{k}}=\sqrt{\frac{\hbar\omega_{\mathbf{k}}}{2\epsilon_0 L}}$. For 3D, we consider a dipole moment $\boldsymbol{\mu}_{01}=\mu_{01}\hat{\mathbf{z}}$ and take the transverse electric field in the direction of $\mathbf{e}_{\mathbf{k}}=-\hat{\boldsymbol{\theta}}$, so that $\mathbf{e}_{\mathbf{k}}\cdot\boldsymbol{\mu}_{01}=\mu_{01}\sin\theta$ and the self energy is

$$\begin{aligned}\Gamma^{3\mathrm{D}}(\varepsilon)&=2i\left(\frac{L}{2\pi}\right)^3 2\pi\int\sin^3\theta d\theta\int k^2dk\frac{\mu_{01}^2\mathcal{E}_k^2}{\varepsilon-\varepsilon_0-\hbar\omega_{\mathbf{k}}+i\eta}\\&=i\frac{\mu_{01}^2}{3\pi^2\epsilon_0\hbar^3c^3}\left[-i\pi(\varepsilon-\varepsilon_0)^3\right]\\&=\frac{\mu_{01}^2}{3\pi\epsilon_0\hbar^3c^3}(\varepsilon-\varepsilon_0)^3\end{aligned}$$

Here, $\mathcal{E}_{\mathbf{k}}=\sqrt{\frac{\hbar\omega_{\mathbf{k}}}{2\epsilon_0 L^3}}$. Note that the ε dependence of the self energy will result in a non-exponential decay. In the FGR region, since the Green's operators $\mathcal{G}(\varepsilon)$ are expected to be a sharp peak at $\varepsilon=\varepsilon_1$, we approximate the self energy by their value $\Gamma(\varepsilon)\approx\Gamma(\varepsilon_1)$

$$\Gamma^{1\mathrm{D}}(\varepsilon)\approx\hbar\kappa^{1\mathrm{D}}=\frac{\mu_{01}^2\Omega}{\epsilon_0 c}, \tag{A10}$$
$$\Gamma^{3\mathrm{D}}(\varepsilon)\approx\hbar\kappa^{3\mathrm{D}}=\frac{\mu_{01}^2\Omega^3}{3\pi\epsilon_0 c^3}. \tag{A11}$$

In the following, we will use κ to represent either $\kappa^{1\mathrm{D}}$ or $\kappa^{3\mathrm{D}}$ and $\Gamma=\hbar\kappa$ depending on context. Therefore, the retarded Green's function is approximated as

$$\mathcal{G}_{11}(\varepsilon)\approx\frac{1}{\varepsilon-\varepsilon_1+i\eta+\frac{i}{2}\Gamma}, \tag{A12}$$
$$\mathcal{G}_{\mathbf{k}1}(\varepsilon)\approx\frac{V_{\mathbf{k}}}{\varepsilon-\varepsilon_0-\hbar\omega_{\mathbf{k}}+i\eta}\frac{1}{\varepsilon-\varepsilon_1+i\eta+\frac{i}{2}\Gamma}. \tag{A13}$$

The total wavefunction can be obtained by the Fourier transform of Green's function $|\psi(t)\rangle=-\frac{1}{2\pi i}\int_{-\infty}^{\infty}d\varepsilon e^{-i(\varepsilon+i\eta)t/\hbar}\mathcal{G}(\varepsilon)|\psi(0)\rangle$ and Cauchy integral

$$C_{1,0}(t)=C_1 e^{-i\frac{\varepsilon_1}{\hbar}t-\frac{\kappa}{2}t}, \tag{A14}$$

$$C_{0,\mathbf{k}}(t)=\frac{C_1V_{\mathbf{k}}/\hbar}{\omega_{\mathbf{k}}-\Omega+i\frac{\kappa}{2}}\left[e^{-i\left(\frac{\varepsilon_0}{\hbar}+\omega_{\mathbf{k}}\right)t}-e^{-i\frac{\varepsilon_1}{\hbar}t-\frac{\kappa}{2}t}\right]. \tag{A15}$$

As must be the case, the population of the excited state decays as

$$|C_{1,0}(t)|^2=|C_{1,0}|^2e^{-\kappa t}. \tag{A16}$$

3. Radiation Field Observables in 1D

While Eq. (A16) express the decay of the electronic excited state, in Sec. V, our primary interest was in the dynamics of the EM field. To that end, we now calculate the expectation value of the radiation intensity $\left\langle \widehat{\mathbf{E}}_{\perp}(x,t)^2 \right\rangle$ and the observed electric field $\left\langle \widehat{\mathbf{E}}_{\perp}(x,t) \right\rangle$ using the electric field operator, Eq. (6) for a 1D system. Eq. (6) suggests that the $\{|0;\mathbf{k}\rangle\}$ manifold is coupled to the $|0;0\rangle$ state and the $\{|1;\mathbf{k}\rangle\}$ manifold is coupled to the $|1;0\rangle$ state. Since $C_{1,\mathbf{k}}(t) \approx 0$, the expectation value can be expressed as

$$\left\langle \widehat{\mathbf{E}}_{\perp}(x,t) \right\rangle = \sum_k i\mathcal{E}_k e^{ikx} C_{0,0}^*(t)\, C_{0,\mathbf{k}}(t) + c.c. \quad \text{(A17)}$$

where $\mathcal{E}_{\mathbf{k}} = \sqrt{\frac{\hbar\omega_{\mathbf{k}}}{2\epsilon_0 L^n}}$. By plugging in the density of state for a 1D system, we have

$$\left\langle \widehat{\mathbf{E}}_{\perp}(x,t) \right\rangle = |C_{0,0}(t)|\, C_1 \frac{\mu_{01}}{4\pi\epsilon_0 c} \int d\omega \frac{\omega}{\omega - \Omega + i\frac{\kappa}{2}} \times \left\{ e^{-i\Omega t - \frac{\kappa}{2}t + i\omega x/c} - e^{-i\omega t + i\omega x/c} \right\} + c.c. \quad \text{(A18)}$$

Then we use a Cauchy integral to carry out the integration over ω

$$\left\langle \widehat{\mathbf{E}}_{\perp}(x,t) \right\rangle = |C_{0,0}(t)|\, C_1 \frac{\mu_{01}}{c\epsilon_0} e^{-\frac{\kappa}{2}\left(t - \frac{|x|}{c}\right)} \theta(ct - |x|) \times \left\{ \Omega \sin\Omega\left(t - \frac{|x|}{c}\right) + \frac{\kappa}{2}\cos\Omega\left(t - \frac{|x|}{c}\right) \right\} \quad \text{(A19)}$$

where the step function θ appears because of the Cauchy integral and we will drop the $\frac{\kappa}{2}$ term since $\kappa \ll \Omega$. Therefore, we obtained the expectation value of the electric field in a 1D system as

$$\left\langle \widehat{\mathbf{E}}_{\perp}(x,t) \right\rangle = |C_{0,0}(t)|\, C_1 \times R(x,t) \sin\Omega\left(t - \frac{|x|}{c}\right) \quad \text{(A20)}$$

where the spatial distribution function is given by

$$R(x,t) = \frac{\Omega\mu_{01}}{c\epsilon_0} e^{-\frac{\kappa}{2}\left(t - \frac{|x|}{c}\right)} \times \theta(ct - |x|). \quad \text{(A21)}$$

For a given time t, we find that $\left\langle \widehat{\mathbf{E}}_{\perp}(x,t) \right\rangle$ oscillates in space at frequency Ω/c and the event horizon can be observed at $|x| = ct$. The magnitude of the electric field can be estimated by $\left\langle \widehat{\mathbf{E}}_{\perp}(x,t) \right\rangle^2$. Here we perform a coarse-grain average over a short time τ, satisfying $2\pi/\Omega \ll \tau \ll 1/\kappa$, and obtain

$$\overline{\left\langle \widehat{\mathbf{E}}_{\perp}(x,t) \right\rangle^2} = \frac{1}{\tau}\int_t^{t+\tau} dt' \left\langle \widehat{\mathbf{E}}_{\perp}(x,t) \right\rangle^2 \quad \text{(A22)}$$

$$= |C_{0,0}(t)|^2 |C_1|^2 \times \frac{R(x,t)^2}{2}, \quad \text{(A23)}$$

In Eq. (A22), we have approximated $\overline{\sin^2\Omega t} \approx \frac{1}{2}$. Within the time scale τ, the population does not change much and the coherence is considered as a rapid oscillation.

Beyond $\left\langle \widehat{\mathbf{E}}_{\perp} \right\rangle^2$, it is standard to evaluate $\left\langle \widehat{\mathbf{E}}_{\perp}^2 \right\rangle$, so as to better understand the nature of quantum fluctuation of the EM field. According to Eq. (6), $\widehat{\mathbf{E}}_{\perp}^2$ operator include only couplings within the manifolds of $\{|0;k\rangle\}$ and $\{|1;k\rangle\}$. Since $\{|1;k\rangle\}$ is the off-resonant manifold, we will ignore the contribution. Therefore, following the same procedure as above, we can obtain the expectation value of the radiation intensity

$$\overline{\left\langle \widehat{\mathbf{E}}_{\perp}^2(x,t) \right\rangle} = |C_1|^2 \times \frac{R(x,t)^2}{2} \quad \text{(A24)}$$

where we ignore vacuum fluctuation of the radiation field. Note that $\left\langle \widehat{\mathbf{E}}_{\perp}^2 \right\rangle \neq \left\langle \widehat{\mathbf{E}}_{\perp} \right\rangle^2$. In fact, most interestingly,

$$\frac{\left\langle \widehat{\mathbf{E}}_{\perp}(x,t) \right\rangle^2}{\left\langle \widehat{\mathbf{E}}_{\perp}^2(x,t) \right\rangle} = |C_{0,0}(t)|^2 \quad \text{(A25)}$$

Appendix B: Derivation of the electric dipole coupling in Ehrenfest dynamics

To derive the electric dipole coupling of the semiclassical electronic Hamiltonian Eq. (20), we need a solution to Maxwell's equation Eqs. (22–23) with the source given by average polarization and average current (Eq. (24)). Here, we will consider a polarization distribution as a delta function at the origin and derive the electric dipole coupling of Ehrenfest dynamics.

In a 3D system, Jefimenko's equations give a general expression of the classical EM field due to an arbitrary charge and current density taking the retardation of the field into account. The retarded electric field in the frequency domain is given by[34]

$$\mathbf{E}_{\omega}(\mathbf{r}) = \frac{1}{4\pi\epsilon_0}\int \mathrm{d}v' e^{iks} \left\{ \frac{\rho'_{\omega}\hat{\mathbf{s}}}{s^2} - ik\frac{\rho'_{\omega}\hat{\mathbf{s}}}{s} + ik\frac{\mathbf{J}'_{\omega}}{cs} \right\} \quad \text{(B1)}$$

where $\mathbf{s} = \mathbf{r} - \mathbf{r}'$ and $\omega = ck$. Here, we denote the Fourier transform of a time-dependent function $f(t)$ as $f_{\omega} = \frac{1}{2\pi}\int f(t) e^{i\omega t} dt$ and write $\rho'_{\omega} = \rho_{\omega}(\mathbf{r}')$ and $\mathbf{J}'_{\omega} = \mathbf{J}_{\omega}(\mathbf{r}')$ for convenience. According to the continuity equation, the retarded field can be written as

$$\mathbf{E}_{\omega}(\mathbf{r}) = \frac{1}{4\pi\epsilon_0}\int \mathrm{d}v' e^{iks} \left\{ -\frac{\boldsymbol{\nabla}'\mathbf{P}'_{\omega}}{s^2}\hat{\mathbf{s}} - \frac{\boldsymbol{\nabla}'\mathbf{J}'_{\omega}}{cs}\hat{\mathbf{s}} + ik\frac{\mathbf{J}'_{\omega}}{cs} \right\}. \quad \text{(B2)}$$

Now, consider the polarization operator $\widehat{\mathbf{P}}(\mathbf{r}) = \boldsymbol{\xi}(\mathbf{r})(|0\rangle\langle 1| + |1\rangle\langle 0|)$, the average polarization ($\mathbf{P}(\mathbf{r},t) = \mathrm{Tr}_s\left\{\widehat{\rho}(t)\widehat{\mathbf{P}}(\mathbf{r})\right\}$) and average current ($\mathbf{J}(\mathbf{r},t) = \frac{\partial}{\partial}\mathbf{P}(\mathbf{r},t)$) can be expressed in the frequency domain as

$$\mathbf{P}_{\omega}(\mathbf{r}) = 2\mathcal{R}_{\omega}\boldsymbol{\xi}(\mathbf{r}) \quad \text{(B3)}$$

$$\mathbf{J}_\omega(\mathbf{r}) = -2\Omega\mathcal{I}_\omega\boldsymbol{\xi}(\mathbf{r}) = -i2\omega\mathcal{R}_\omega\boldsymbol{\xi}(\mathbf{r}) \tag{B4}$$

where we define $\mathcal{R}_\omega = \mathrm{Re}\left[\rho_{01}\right]_\omega$ and $\mathcal{I}_\omega = \mathrm{Im}\left[\rho_{01}\right]_\omega$.

We would like to calculate the electric dipole coupling:

$$H_{01}^{\mathrm{el}} = -\int d\omega e^{-i\omega t}\int \mathrm{d}\mathbf{r}\mathbf{E}_\omega\cdot\boldsymbol{\xi} \tag{B5}$$

where the spatial integration is

$$\begin{aligned}\int \mathrm{d}\mathbf{r}\mathbf{E}_\omega\cdot\boldsymbol{\xi} =& \frac{\mathcal{R}_\omega}{2\pi\epsilon_0}\int \mathrm{d}v\int \mathrm{d}v' e^{iks} \\ & \left\{-\frac{\boldsymbol{\nabla}'\cdot\boldsymbol{\xi}'}{s^2}\xi_s + i\omega\frac{\boldsymbol{\nabla}'\cdot\boldsymbol{\xi}'}{cs}\xi_s + \frac{\omega^2\boldsymbol{\xi}\cdot\boldsymbol{\xi}'}{c^2 s},\right\}\end{aligned} \tag{B6}$$

and $\xi_s = \boldsymbol{\xi}(\mathbf{r})\cdot\hat{\mathbf{s}}$. The spatial integration can be carried out using integration by part and eliminating boundary contributions:

$$\begin{aligned}&-\int \mathrm{d}v' e^{iks}\frac{\boldsymbol{\nabla}'\cdot\boldsymbol{\xi}'}{s^2}\xi_s \\ &= \int \mathrm{d}v'\boldsymbol{\xi}'\cdot\boldsymbol{\nabla}'\frac{\xi_s e^{iks}}{s^2} \\ &= \int \mathrm{d}v' e^{iks}\left[-\frac{ik}{s^2}\xi_s\xi_s' + \frac{2}{s^3}\xi_s\xi_s' + \frac{1}{s^2}\boldsymbol{\xi}'\cdot\boldsymbol{\nabla}'\xi_s\right]\end{aligned}$$

$$\begin{aligned}&i\omega\int \mathrm{d}v'\frac{\boldsymbol{\nabla}'\cdot\boldsymbol{\xi}'}{cs}\xi_s e^{iks} \\ &= -ik\int \mathrm{d}v'\boldsymbol{\xi}'\cdot\boldsymbol{\nabla}'\frac{\xi_s e^{iks}}{s} \\ &= \int \mathrm{d}v' e^{iks}\left[-\frac{k^2}{s}\xi_s\xi_s' - \frac{ik}{s^2}\xi_s\xi_s' - \frac{ik}{s}\boldsymbol{\xi}'\cdot\boldsymbol{\nabla}'\xi_s\right]\end{aligned}$$

Therefore,

$$\begin{aligned}\int \mathrm{d}v\mathbf{E}_\omega\cdot\boldsymbol{\xi} =& \frac{\mathcal{R}_\omega}{2\pi\epsilon_0}\int \mathrm{d}v\int \mathrm{d}v' e^{iks} \\ & \left\{\left(-2\frac{ik}{s^2} + \frac{2}{s^3} - \frac{k^2}{s}\right)\xi_s\xi_s' + \right. \\ & \left.\left(\frac{1}{s^2} - \frac{ik}{s}\right)\boldsymbol{\xi}'\cdot\boldsymbol{\nabla}'\xi_s + \frac{k^2}{s}\boldsymbol{\xi}\cdot\boldsymbol{\xi}'\right\}\end{aligned} \tag{B7}$$

To be explicit, we assume that the source distribution is a delta function at the origin without dependence on either θ or ϕ, and polarized in the z direction:

$$\boldsymbol{\xi}(\mathbf{r}') = \mu_{01}\delta^3(r')\hat{\mathbf{z}}, \tag{B8}$$

where $\delta^3(r')$ is a 3D delta function and $r' = |\mathbf{r}'|$. Because we only consider $\mathbf{r}\approx\mathbf{r}'\approx 0$ in the above integral, we can approximate

$$\boldsymbol{\xi}(\mathbf{r}) = \mu_{01}\delta^3(|\mathbf{r}'+\mathbf{s}|)\hat{\mathbf{z}} \approx \mu_{01}\delta^3(|\mathbf{s}|)\hat{\mathbf{z}} = \mu_{01}\delta^3(s)\hat{\mathbf{z}}. \tag{B9}$$

Now we transform the integral by $\int \mathrm{d}v\int \mathrm{d}v' \rightarrow \int \mathrm{d}v'\int \mathrm{d}s\mathrm{d}\theta\mathrm{d}\phi s^2\sin\theta$ and use $\xi_s \approx \mu_{01}\delta^3(s)\cos\theta$, $\xi_s' = \mu_{01}\delta^3(r')\cos\theta$, and $\boldsymbol{\xi}'\cdot\boldsymbol{\nabla}'\xi_r \approx -\mu_{01}^2\delta^3(r')\delta^3(s)\sin^2\theta/s$. After carrying the θ and ϕ integration in the spherical coordinate and $\int \mathrm{d}\mathbf{r}'\delta^3(r') = 1$, we obtain

$$\int \mathrm{d}v\mathbf{E}_\omega\cdot\boldsymbol{\xi} = \frac{\mu_{01}^2\mathcal{R}_\omega k^2}{3\pi\epsilon_0}\int_0^\infty ds\delta(s)\frac{e^{iks}}{s} \tag{B10}$$

where all the $1/s^2$ and $1/s^3$ terms are canceled out. The radial integration of Eq. (B10) gives

$$\int_0^\infty ds\delta(s)\frac{e^{iks}}{s} = \lim_{\eta\to 0}\frac{1}{\eta} + ik, \tag{B11}$$

where the real part of the integral is infinite but not depends on k. When plugging into Eq. (B5), the real part turns out to be $\lim_{\eta\to 0}\frac{1}{\eta}\delta(t)$ which represent a self-interaction at $t = 0$. So we may ignore it.

Finally, by Eq. (B5) and approximating $ik^3\mathcal{R}_\omega = \dddot{\mathcal{R}}_\omega/c^3 \approx \Omega^3\mathcal{I}/c^3$, we can write the electric dipole coupling

$$H_{01}^{\mathrm{el}} = -\frac{\mu_{01}^2\Omega^3}{3\pi\epsilon_0 c^3}\mathcal{I} = -\hbar\kappa^{3\mathrm{D}}\mathrm{Im}\rho_{01} \tag{B12}$$

Appendix C: The direction of the rescaling field

1. The 3D case

Here, we provide numerical proof that $\delta\mathbf{E}_R = \boldsymbol{\nabla}\times\boldsymbol{\nabla}\times\mathbf{P}$ and $\delta\mathbf{B}_R = \boldsymbol{\nabla}\times\mathbf{P}$ are an appropriate rescaling directions for spontaneous emission. To do so, we run Ehrenfest dynamics for the 3D system in Sec. V. We calculate the overlap of the Ehrenfest EM field arising from the origin (where$\mathbf{P}^{3\mathrm{D}} \neq 0$) with $\boldsymbol{\nabla}\times\boldsymbol{\nabla}\times\mathbf{P}^{3\mathrm{D}}$and $\boldsymbol{\nabla}\times\mathbf{P}^{3\mathrm{D}}$. To be precise, consider a spherical shell outside of the region of $\mathbf{P}^{3\mathrm{D}}(\mathbf{r})$. We calculate the normalized overlap estimation in this region defined as

$$(\mathbf{E}_{Eh}|\delta\mathbf{E}_R) = \frac{\int_\circledcirc \mathrm{d}v\mathbf{E}_{Eh}\cdot\delta\mathbf{E}_R}{\sqrt{\int_\circledcirc \mathrm{d}v\left|\mathbf{E}_{Eh}\right|^2\int_\circledcirc \mathrm{d}v\left|\delta\mathbf{E}_R\right|^2}} \tag{C1}$$

where $\int_\circledcirc \mathrm{d}v$ denote the integral within the spherical shell. If our intuition is correct, the overlap should be large and oscillatory as the emanated wave propagates out into free space.

In Fig. (4), we plot the normalized overlap for short times. We consider a Gaussian distribution of width about 3 nm. The overlap of magnetic fields exhibit an oscillatory behavior in the near and far field. However, the overlap of electric field shows similar behavior only in the far field. It is attributed to the fact that the electric field have a more complicated near field component. Despite this, we find that, when the emission field begins to enter the vacuum ($t < 0.05$ fs), $\left(\mathbf{E}_{Eh}|\left(\boldsymbol{\nabla}\times\right)^2\mathbf{P}^{3\mathrm{D}}\right)$ and $\left(\mathbf{B}_{Eh}|\boldsymbol{\nabla}\times\mathbf{P}^{3\mathrm{D}}\right)$ account for more than 90% of the emission field in the near field. This data then strongly

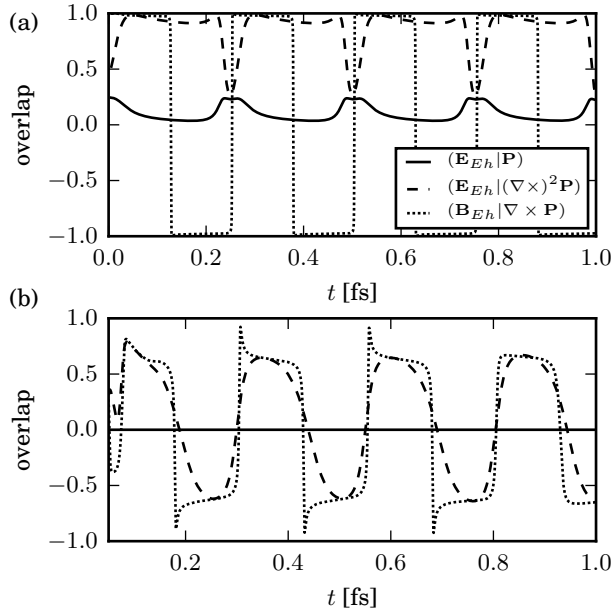

Figure 4. The normalized overlap of the EM field of Ehrenfest dynamics a function of time in 3D space. The initial state of Ehrenfest dynamics is $|\psi\rangle = \sqrt{\frac{1}{2}}|0\rangle + \sqrt{\frac{1}{2}}|1\rangle$. The solid line is the overlap of $(\mathbf{E}_{Eh}|\mathbf{P})$, the dash line is the overlap of $\left(\mathbf{E}_{Eh}|\left(\boldsymbol{\nabla}\times\right)^2\mathbf{P}\right)$, and the dotted line is the overlap of $(\mathbf{B}_{Eh}|\boldsymbol{\nabla}\times\mathbf{P})$. The shell radius are (a) $6.0-7.5$ nm and (b) $30.0-31.5$ nm. Note that the data shows that $\left(\boldsymbol{\nabla}\times\right)^2\mathbf{P}$ and $\boldsymbol{\nabla}\times\mathbf{P}$ should be the leading order contributions to the rescaling field for E and B fields respectively.

suggest that the leading order contributions to the rescaling field should be in the direction of $\delta\mathbf{E}_R = \left(\boldsymbol{\nabla}\times\right)^2\mathbf{P}^{3\mathrm{D}}$ for the electric field and $\delta\mathbf{B}_R = \boldsymbol{\nabla}\times\mathbf{P}^{3\mathrm{D}}$ for the magnetic field.

2. The 1D case

Interestingly, the analysis above is less straightforward in 1D. Here we consider a polarization distribution given by Eq. (51) and the width of Gaussian distribution is assumed to be much smaller than the wavelength ($\frac{1}{\sqrt{a}} \ll \frac{2\pi c}{\Omega}$). Compared to the 3D case, $\boldsymbol{\nabla}\times\boldsymbol{\nabla}\times\mathbf{P}^{1\mathrm{D}}$ and $\boldsymbol{\nabla}\times\mathbf{P}^{1\mathrm{D}}$ overlap with $\mathbf{P}^{1\mathrm{D}}$ can not be ignored. For a 1D system, the overlap leads to unwanted EM fields propagating back to the origin.

To circumvent this issue, we add additional transverse field to the rescaling field as a simplest prescription:

$$\delta\mathbf{E}_R = \boldsymbol{\nabla}\times\boldsymbol{\nabla}\times\mathbf{P}^{1\mathrm{D}} - g\mathbf{P}^{1\mathrm{D}}, \tag{C2}$$

$$\delta\mathbf{B}_R = \boldsymbol{\nabla}\times\mathbf{P}^{1\mathrm{D}} - h\left(\boldsymbol{\nabla}\times\right)^3\mathbf{P}^{1\mathrm{D}}, \tag{C3}$$

where the coefficients g and h are determined by $\delta\mathbf{E}_R(x=0) = 0$ and $\boldsymbol{\nabla}\times\delta\mathbf{B}_R(x=0) = 0$. Here, a straightforward choice of the additional field are obtained by iterating Maxwell's equation. Since the average current has the same spatial distribution with $\mathbf{P}^{1\mathrm{D}}$, the E field derived from Maxwell's equations is a linear combination of $\mathbf{P}^{1\mathrm{D}}$ and even order derivatives of $\mathbf{P}^{1\mathrm{D}}$. Also, the B field is a linear combination of the odd derivatives of $\mathbf{P}^{1\mathrm{D}}$.

Specifically, for Eq. (51), $g = 2a$ and $h = 1/6a$, and the rescaling field is

$$\delta\mathbf{E}_R(x) = -4a^2x^2e^{-ax^2}\mu_{01}\sqrt{\frac{a}{\pi}}\hat{\mathbf{z}}, \tag{C4}$$

$$\delta\mathbf{B}_R(x) = \frac{4}{3}a^2x^3e^{-ax^2}\mu_{01}\sqrt{\frac{a}{\pi}}\hat{\mathbf{y}}. \tag{C5}$$

Appendix D: Derivation of the rescaling factors α^ℓ and β^ℓ

In an ideal world, one would like to enforce energy conservation for every trajectory, much in the same way as Tully's FSSH algorithm operates. Thus, every time an electron is forced to relax, one would like to insert increase the energy in the EM field so as to satisfy conservation of energy:

$$\begin{aligned}\delta U_R = &\frac{\epsilon_0}{2}\int \mathrm{d}v\left(2\mathbf{E}_{Eh}\cdot\alpha\delta\mathbf{E}_R + |\alpha\delta\mathbf{E}_R|^2\right)\\ &+\frac{1}{2\mu_0}\int \mathrm{d}v\left(2\mathbf{B}_{Eh}\cdot\beta\delta\mathbf{B}_R + |\beta\delta\mathbf{B}_R|^2\right).\end{aligned} \tag{D1}$$

To satisfy requirement (c), we assume the E and B rescaling field carry equal energy density so that Eq. (D1) becomes two independent quadratic equations:

$$\frac{\delta U_R}{2} = \frac{\epsilon_0}{2}\int \mathrm{d}v\left(2\mathbf{E}_{Eh}\cdot\alpha\delta\mathbf{E}_R + |\alpha\delta\mathbf{E}_R|^2\right) \tag{D2}$$

$$= \frac{1}{2\mu_0}\int \mathrm{d}v\left(2\mathbf{B}_{Eh}\cdot\beta\delta\mathbf{B}_R + |\beta\delta\mathbf{B}_R|^2\right) \tag{D3}$$

Note that, since $\delta U_R\int \mathrm{d}v\,|\delta\mathbf{E}_R|^2 > 0$ and $\delta U_R\int \mathrm{d}v\,|\delta\mathbf{B}_R|^2 > 0$, the solution of the quadratic equation must have opposite signs. Also, to ensure the Poynting vector of the rescaling field is outward, we choose the solution of α and β with the same sign as $\mathrm{sgn}\left(\mathrm{Im}\left[\rho_{01}e^{i\phi}\right]\right)$ for a random phase.

Unfortunately, however, one can easily discern that this ansatz is unworkable. To see this, note that the choice of α and β cause the rescaling field invert when the sign of $\mathrm{Im}\left[\rho_{01}e^{i\phi}\right]$ changes. After enforcing energy conservation, inverting the rescaling field at random time would lead to chaotic EM dynamics (see Fig. 5(b) and (c)). Moreover, when the emission is dominated by the rescaling field (i.e. $\rho_{11}\approx 1$) and out of phase ($\phi = \pi$), the electric field has been completely inverted and is nonsensical. If we would always choose the in-phase solution (Fig. 5(a)) and we would find a large, coherent outgoing electric field, with $\langle\mathbf{E}^2\rangle = \langle\mathbf{E}\rangle^2$. And yet, as we know from Appendix A, this solution is also incorrect.

In the end, our intuition is that one cannot capture the essence of spontaneous emission by enforcing energy

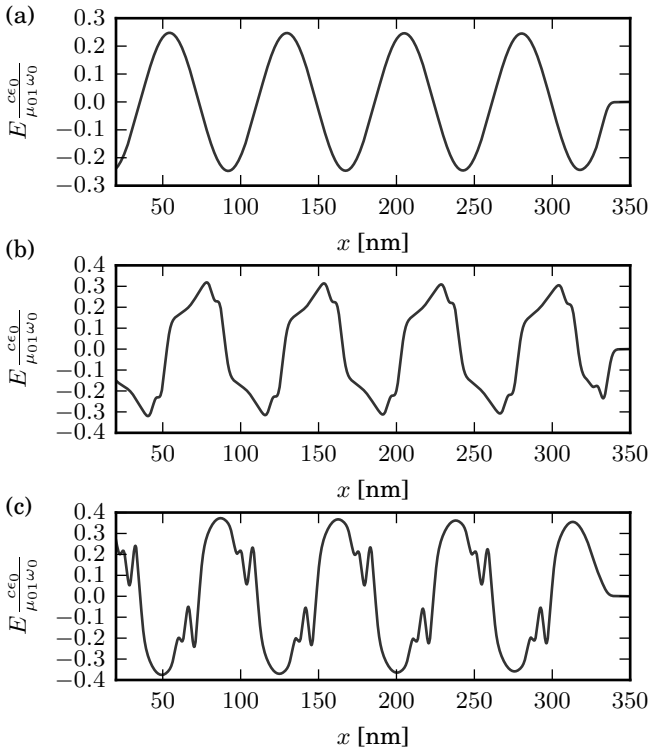

Figure 5. The electric field produced for spontaneous emission in 1D as a function of x at $t = 1.1$ fs by Ehrenfest+R method enforcing energy conservation. The phases of the rescaling field are chosen to be (a) $\phi = 0$, (b) $\phi = 0.5\pi$, and (c) $\phi = \pi$. The initial condition is $\rho_{11} = 0.9$. Note that inverting the electric field out of phase in (b) and (c) leads to unphysical pulses of the EM field. Also note that the electric field in (c) is completely inverted to (a).

conservation for each trajectory; instead, energy conservation can be enforced only on average. Note that this ansatz agrees with a host of work modeling nuclear quantum effects with interacting trajectories designed to reproduce the Wigner distribution. To that end, we emphasize that true spontaneous emission requires quantum (not classical) photons (bosons); this is not the same problem as the FSSH problem, where one is dealing with a classical nuclei (bosons).

Now, in order to enforce energy conservation on average, imagine that we run N_{traj} trajectories (indexed by ℓ), and for each trajectory, the EM field is written as the pure Ehrenfest EM fields plus a sum of N_{traj} rescaling fields of each retarded time steps jdt:

$$\mathbf{E}^{\ell}_{Eh+R}(t) = \mathbf{E}^{\ell}_{Eh}(t) + \sum_{j=0}^{n} \alpha^{\ell}_{j} \delta\mathbf{E}_R(t - jdt) \quad \text{(D4)}$$

$$\mathbf{B}^{\ell}_{Eh+R}(t) = \mathbf{B}^{\ell}_{Eh}(t) + \sum_{j=0}^{n} \beta^{\ell}_{j} \delta\mathbf{B}_R(t - jdt) \quad \text{(D5)}$$

where $\delta\mathbf{E}_R(\Delta t)$ and $\delta\mathbf{B}_R(\Delta t)$ are the rescaling field propagating for Δt according to Maxwell's equations. For the last time step ($t = ndt$), energy conservation must satisfy the following condition:

$$\begin{aligned}\left\langle \delta U^{\ell}_R \right\rangle = &\frac{\epsilon_0}{2}\int \mathrm{d}v \left\langle 2\mathbf{E}^{\ell}_{Eh}(t)\cdot\alpha^{\ell}_n\delta\mathbf{E}_R\right\rangle \\ &+\frac{\epsilon_0}{2}\int \mathrm{d}v \left\langle 2\sum_{j=0}^{n-1}\alpha^{\ell}_j\delta\mathbf{E}_R(t-jdt)\cdot\alpha^{\ell}_n\delta\mathbf{E}_R\right\rangle \\ &+\frac{\epsilon_0}{2}\int \mathrm{d}v \left\langle \left|\alpha^{\ell}_n\delta\mathbf{E}_R\right|^2\right\rangle \\ &+\frac{1}{2\mu_0}\int \mathrm{d}v \left\langle 2\mathbf{B}^{\ell}_{Eh}(t)\cdot\beta^{\ell}_n\delta\mathbf{B}_R\right\rangle \\ &+\frac{1}{2\mu_0}\int \mathrm{d}v \left\langle 2\sum_{j=0}^{n-1}\beta^{\ell}_j\delta\mathbf{B}_R(t-jdt)\cdot\beta^{\ell}_n\delta\mathbf{B}_R\right\rangle \\ &+\frac{1}{2\mu_0}\int \mathrm{d}v \left\langle \left|\beta^{\ell}_n\delta\mathbf{B}_R\right|^2\right\rangle \quad \text{(D6)}\end{aligned}$$

where $\langle\cdots\rangle = \frac{1}{N_{\text{traj}}}\sum_{\ell}^{N_{\text{traj}}}$. Now, let us assume that there is phase cancellation between different trajectories, i.e. $\left\langle \mathbf{E}^{\ell}_{Eh}(t)\cdot\alpha^{\ell}_n\delta\mathbf{E}_R\right\rangle = \left\langle \mathbf{B}^{\ell}_{Eh}(t)\cdot\beta^{\ell}_n\delta\mathbf{B}_R\right\rangle = 0$.

Although the cross term between the pure Ehrenfest field and the rescaling fields can be eliminated by phase cancellation, the rescaling fields of current time step ($j = n$) and that from previous times ($j < n$) still have non-vanish cross terms on average. From Eq. (D6), we note that the cross term is associated with the overlaps $\int \mathrm{d}v\delta\mathbf{E}_R(t-jdt)\cdot\delta\mathbf{E}_R$ and $\int \mathrm{d}v\delta\mathbf{B}_R(t-jdt)\cdot\delta\mathbf{B}_R$. At this point, we presume that $\alpha^{\ell}_j \approx \alpha^{\ell}_n$ and $\beta^{\ell}_j \approx \beta^{\ell}_n$ does not change much for a short time and Eq. (D6) can be simplified as

$$\begin{aligned}\left\langle \delta U^{\ell}_R\right\rangle = &\frac{\Lambda_E(t)}{cdt}\frac{\epsilon_0}{2}\int \mathrm{d}v\left\langle\left|\alpha^{\ell}_n\delta\mathbf{E}_R\right|^2\right\rangle \\ &+\frac{\Lambda_B(t)}{cdt}\frac{1}{2\mu_0}\int \mathrm{d}v\left\langle\left|\beta^{\ell}_n\delta\mathbf{B}_R\right|^2\right\rangle \quad \text{(D7)}\end{aligned}$$

where we define the self-interference length Λ_E and Λ_B corresponding to $\delta\mathbf{E}_R$ and $\delta\mathbf{B}_R$, respectively:

$$\frac{\Lambda_E(t)}{cdt} = 1 + \frac{2\int \mathrm{d}v\sum_{j=0}^{n-1}\delta\mathbf{E}_R(t-jdt)\cdot\delta\mathbf{E}_R}{\int \mathrm{d}v\left|\delta\mathbf{E}_R\right|^2} \quad \text{(D8)}$$

$$\frac{\Lambda_B(t)}{cdt} = 1 + \frac{2\int \mathrm{d}v\sum_{j=0}^{n-1}\delta\mathbf{B}_R(t-jdt)\cdot\delta\mathbf{B}_R}{\int \mathrm{d}v\left|\delta\mathbf{B}_R\right|^2} \quad \text{(D9)}$$

These quantities must mimic the spatial size of $\delta\mathbf{E}_R = \boldsymbol{\nabla}\times\boldsymbol{\nabla}\times\mathbf{P}$ and $\delta\mathbf{B}_R = \boldsymbol{\nabla}\times\mathbf{P}$ and will reach a constant in a short time. In practice, we can use $\Lambda_E(t) \to \Lambda_E$ and $\Lambda_B(t) \to \Lambda_B$ for all time.

Now we impose the assumption that the E and B rescaling field carry equal energy density (i.e. $\frac{\epsilon_0}{2}\int \mathrm{d}v\left\langle\left|\alpha^{\ell}_n\delta\mathbf{E}_R\right|^2\right\rangle = \frac{1}{2\mu_0}\int \mathrm{d}v\left\langle\left|\beta^{\ell}_n\delta\mathbf{B}_R\right|^2\right\rangle$), so that energy conservation Eq. (D7) can further simplify:

$$\frac{\left\langle \delta U^{\ell}_R\right\rangle}{2} = \frac{\Lambda}{cdt}\frac{\epsilon_0}{2}\int \mathrm{d}v\left\langle\left|\alpha^{\ell}_n\delta\mathbf{E}_R\right|^2\right\rangle \quad \text{(D10)}$$

$$= \frac{\Lambda}{cdt}\frac{1}{2\mu_0}\int \mathrm{d}v\left\langle\left|\beta^{\ell}_n\delta\mathbf{B}_R\right|^2\right\rangle \quad \text{(D11)}$$

where the average self-interference length is $\Lambda = (\Lambda_E + \Lambda_B)/2$.

Finally, α_n^ℓ and β_n^ℓ are determined by

$$\alpha_n^\ell = \sqrt{\frac{cdt}{\Lambda}\frac{\delta U_R^\ell}{\epsilon_0 \int \mathrm{d}v \left|\delta \mathbf{E}_R\right|^2}} \times \mathrm{sgn}\left(\mathrm{Im}\left[\rho_{01} e^{i\phi^\ell}\right]\right) \quad \text{(D12)}$$

$$\beta_n^\ell = \sqrt{\frac{cdt}{\Lambda}\frac{\mu_0 \delta U_R^\ell}{\int \mathrm{d}v \left|\delta \mathbf{B}_R\right|^2}} \times \mathrm{sgn}\left(\mathrm{Im}\left[\rho_{01} e^{i\phi^\ell}\right]\right) \quad \text{(D13)}$$

where the sign is chosen according to the +R relaxation rate k_R, Eq. (33). Here, the choice ensure phase cancellation between different trajectories (i.e. $\langle \alpha_n^\ell \rangle = \langle \beta_n^\ell \rangle = 0$) due to the random phase ϕ^ℓ. Note that Ehrenfest+R trajectories has a random phase shift from the Ehrenfest EM field which oscillating together with $\mathrm{Im}[\rho_{01}]$. Therefore, the rescaling field leads to destructive or constructive interference to $\mathbf{E}_{Eh}$ depending on ϕ^ℓ.

REFERENCES

[1] R. J. Thompson, Physical Review A **57**, 3084 (1998).
[2] E. Solano, G. S. Agarwal, and H. Walther, Phys. Rev. Lett. **90**, 027903 (2003).
[3] J. M. Fink, M. Göppl, M. Baur, R. Bianchetti, P. J. Leek, A. Blais, and A. Wallraff, Nature **454**, 315 (2008).
[4] P. T{\"o}rm{\"a} and W. L. Barnes, Reports on Progress in Physics **78**, 013901 (2015).
[5] R. Puthumpally-Joseph, M. Sukharev, O. Atabek, and E. Charron, Physical Review Letters **113**, 163603 (2014).
[6] R. Puthumpally-Joseph, O. Atabek, M. Sukharev, and E. Charron, Physical Review A **91**, 043835 (2015).
[7] M. Sukharev and A. Nitzan, Journal of Physics: Condensed Matter **29**, 443003 (2017).
[8] R. H. Dicke, Physical Review **93**, 99 (1954).
[9] A. V. Andreev, V. I. Emel'yanov, and Y. A. Il'inskiĭ, Soviet Physics Uspekhi **23**, 493 (1980).
[10] S. Oppel, R. Wiegner, G. S. Agarwal, and J. von Zanthier, Physical Review Letters **113**, 263606 (2014).
[11] P. a. M. Dirac, Proc. R. Soc. Lond. A **114**, 710 (1927).
[12] P. a. M. Dirac, Proc. R. Soc. Lond. A **114**, 243 (1927).
[13] P. W. Milonni, Physics Reports **25**, 1 (1976).
[14] W. H. Miller, *Classical limit quantum mechanics and the theory of molecular collisions*, Vol. 25 (1974).
[15] R. Kapral and G. Ciccotti, J. Chem. Phys. **110**, 8919 (1999).
[16] J. C. Tully, Faraday Discuss. **110**, 407 (1998).
[17] J. C. Tully, The Journal of Chemical Physics **93**, 1061 (1990).
[18] R. W. Ziolkowski, J. M. Arnold, and D. M. Gogny, Physical Review A **52**, 3082 (1995).
[19] G. Slavcheva, J. M. Arnold, I. Wallace, and R. W. Ziolkowski, Physical Review A **66**, 063418 (2002).
[20] A. Fratalocchi, C. Conti, and G. Ruocco, Physical Review A **78**, 013806 (2008).
[21] M. Sukharev and A. Nitzan, Physical Review A **84**, 043802 (2011).
[22] W. H. Miller, The Journal of Chemical Physics **69**, 2188 (1978).
[23] T. E. Li, A. Nitzan, M. Sukharev, T. Martinez, H.-T. Chen, and J. E. Subotnik, arXiv:1801.07154 [physics, physics:quant-ph] (2018), arXiv: 1801.07154.
[24] P. V. Parandekar and J. C. Tully, Journal of Chemical Theory and Computation **2**, 229 (2006).
[25] A. Jain and J. E. Subotnik, The Journal of Physical Chemistry A **122**, 16 (2018).
[26] V. Weisskopf and E. Wigner, Zeitschrift für Physik **63**, 54 (1930).
[27] M. O. Scully and M. S. Zubairy, *Quantum Optics* (Cambridge University Press, 1997) google-Books-ID: 20ISsQCKKmQC.
[28] E. A. Power and S. Zienau, Phil. Trans. R. Soc. Lond. A **251**, 427 (1959).
[29] P. W. Atkins and R. G. Woolley, Proc. R. Soc. Lond. A **319**, 549 (1970).
[30] C. Cohen-Tannoudji, J. Dupont-Roc, and G. Grynberg, *Photons and Atoms: Introduction to Quantum Electrodynamics* (1997).
[31] A. Nitzan, *Chemical Dynamics in Condensed Phases: Relaxation, Transfer, and Reactions in Condensed Molecular Systems* (Oxford University Press, New York, 2006).
[32] S. Mukamel, *Principles of Nonlinear Optics and Spectroscopy* (Oxford University Press, 1999).
[33] Since there is no decoherence introduced, the off-diagonal element of $\mathcal{L}_R\rho$ is obtained by conversing the purity of density matrix. i.e. $\frac{d}{dt}(\rho_{00}\rho_{11} - |\rho_{01}|^2) = 0$.
[34] W. K. H. Panofsky and j. a. Phillips, Melba, *Classical electricity and magnetism*, 2nd ed. (Reading, Mass Addison-Wesley Pub. Co, 1962).